Zoological Journal of the Linnean Society, 2024, **202**, zlae109
https://doi.org/10.1093/zoolinnean/zlae109
Advance access publication 9 October 2024
Original Article

OXFORD

Original Article

New theropod dinosaur remains from the Upper Cretaceous of the Kem Kem Group (Eastern Morocco) clarify spinosaurid morphology

Mauro B.S. Lacerda[*,1–3], Erik Isasmendi[4,5], Rafael Delcourt[6,7], Marcelo A. Fernandes[1] and John R. Hutchinson[2]

[1]Departamento de Ecologia e Biologia Evolutiva (DEBE), Universidade Federal de São Carlos (UFSCar), São Carlos, 13565–905, Brazil
[2]Structure and Motion Laboratory, Department of Comparative Biomedical Sciences, The Royal Veterinary College (RVC), Hatfield, AL9 7TA, United Kingdom
[3]Pós-Graduação em Zoologia, Instituto de Ciências Biológicas, Universidade Federal de Minas Gerais (UFMG), Belo Horizonte, 31270–901, Brazil
[4]Departamento de Geología/Geologia Saila, Facultad de Ciencia y Tecnología/Zientzia eta Teknologia Fakultatea, Universidad del País Vasco/Euskal Herriko Unibertsitatea, Leioa, 48940, Spain
[5]Centro de Interpretación Paleontológica de La Rioja, Igea, 26525, Spain
[6]Laboratório de Paleontologia, Faculdade de Filosofia, Ciências e Letras de Ribeirão Preto, Universidade de São Paulo (USP), Ribeirão Preto, 14040–901, Brazil
[7]Bayerische Staatssammlung für Paläontologie und Geologie (SNSB), Department of Earth and Environmental Sciences, GeoBioCenter, Ludwig-Maximilians-University, München, D–80333, Germany

[*]Corresponding author. Departamento de Ecologia e Biologia Evolutiva (DEBE), Universidade Federal de São Carlos (UFSCar), São Carlos-SP, 13565–905, Brazil.
Email address: mlacerda@ufscar.br

ABSTRACT

The Kem Kem Group is a lowermost lithostratigraphic unit from the Upper Cretaceous that extends along the border between Algeria and Morocco, in the northern region of Africa. This geological unit has yielded several tetrapod fossils, including a well-represented assemblage of theropod dinosaurs, after more than eight decades of research. Here, we report new occurrences of spinosaurid theropods from the spinosaurine clade in the Kem Kem Group by providing anatomical descriptions and taxonomic identifications of 11 new specimens derived from the Tafilalt region of Morocco. Among the findings, we describe a cervical vertebra of *Sigilmassasaurus*, in addition to several cranial, axial, and appendicular elements that can safely be attributed to Spinosaurinae. Moreover, based on a unique combination of characteristics, we also describe an isolated and partial ischium belonging to an indeterminate carcharodontosaurid. We also deliver a detailed redescription of one of the most complete snouts of a spinosaurine known to date. Therefore, the theropod dinosaurs of the Kem Kem Group show considerable diversity, but many questions, especially related to the diversity of spinosaurids and the general abundance of carnivorous dinosaurs in this region, remain unclear until new materials are discovered and complete descriptions are made.

Keywords: Africa; Cretaceous; Dinosauria; Theropoda

INTRODUCTION

Several fossil assemblages from Morocco and Algeria (the edge of the Sahara Desert) in the north-western region of continental Africa present a great diversity of fossil vertebrate fauna. This fauna derives from a palaeoenvironment of rivers and alluvial plains known as the Kem Kem Group (*sensu* Ibrahim *et al.* 2020b), but also commonly referred to as Kem Kem beds and also known as 'Kem Kem compound assemblages' or Kem Kem plateau (Sereno *et al.* 1996, Cavin *et al.* 2010, Belvedere *et al.* 2013, Benyoucef *et al.* 2015, Alloul *et al.* 2018, Ibrahim *et al.* 2020b). The Kem Kem Group is generally considered to be Upper Cretaceous, predominantly Cenomanian (Cavin *et al.* 2010, Ibrahim *et al.* 2020b). This unit can be considered a *Konzentrat-Lagerstätte* due to the great accumulation and abundance of vertebrate fossil material (Cavin *et al.* 2010, Smith *et al.* 2023b).

Received 10 May 2024; revised 29 July 2024; accepted 14 August 2024

In these deposits a mixture of terrestrial and volant vertebrates, and freshwater or brackish aquatic vertebrates have been recovered, and within this fauna there appears to be a tendency towards a greater abundance of large carnivorous taxa if compared to other tetrapod taxa (McGowan and Dyke 2009, Cavin *et al.* 2010, Belvedere *et al.* 2013). Although some studies consider the fossil record of the Kem Kem Group to be reliable and representative of the broad diversity and dominance of theropods in the Cenomanian stage of the region, other studies contend that there is a biased perception of the abundance and diversity of theropods that is related to the geological collection bias or the so-called 'Stromer's Riddle' (McGowan and Dyke 2009, Cavin *et al.* 2010, Belvedere *et al.* 2013, Ibrahim *et al.* 2020b).

The vertebrate fossils in the Kem Kem Group derive from several fossiliferous localities (mainly from south-eastern Morocco) located across 250 km distance, and from which more than 80 vertebrate taxa that have been recognized over more than eight decades of palaeontological research (Choubert 1948, Russel 1996, Cavin *et al.* 2010, Ibrahim *et al.* 2020b). As an example of this diversity, the vertebrates of these deltaic deposits include a plethora of taxa, such as cartilaginous and bony fishes (e.g. Cavin *et al.* 2010, Benyoucef *et al.* 2015), amphibians (e.g. Alloul *et al.* 2018, Lemierre and Blackburn 2022), turtles (e.g. Gaffney *et al.* 2002), plesiosaurs (e.g. Bunker *et al.* 2022), snakes (e.g. Klein *et al.* 2017, Vullo 2019), pterosaurs (e.g. Smith *et al.* 2023a), crocodyliforms (e.g. Sereno and Larsson 2009), dinosaurs (e.g. Russell 1996, Mannion and Barrett 2013, Hendrickx *et al.* 2024), and a possible avialan (Riff *et al.* 2004, Cavin *et al.* 2010). Furthermore, ichnological data also show the wide diversity and abundance of vertebrate records in this region (e.g. Belvedere *et al.* 2013, Ibrahim *et al.* 2014b).

Notably, the Kem Kem Group has yielded several large-bodied carnivorous theropod dinosaur taxa, mainly averostrans. Nevertheless, rather than body fossils, the theropod record is mostly represented by isolated teeth (e.g. Amiot *et al.* 2004, Ritcher *et al.* 2013, Benyoucef *et al.* 2015, Hendrickx *et al.* 2024), and isolated bones and a few articulated elements (Russell 1996, Chiarenza and Cau 2016). At least five theropod lineages, including abelisaurids, noasaurids, spinosaurids, carcharodontosaurids, and dromaeosaurids, have been recovered from the Kem Kem Group (Russell 1996, Sereno *et al.* 1996, Taquet and Russell 1998, Milner 2003, Dal Sasso *et al.* 2005, Ritcher *et al.* 2013, Benyoucef *et al.* 2015, Evans *et al.* 2015, Evers *et al.* 2015, Hendrickx *et al.* 2016, 2024, Ibrahim *et al.* 2020b, Smyth *et al.* 2020a). However, it is possible that the purported isolated dromaeosaurid teeth actually belong to noasaurid theropods (Hendrickx *et al.* 2016). The coexistence of more than one large carnivorous species of the same or different clades in the Cenomanian Kem Kem Group can probably be explained by niche partitioning in (micro)habitats (e.g. Hassler *et al.* 2018).

Here, we report on, and provide detailed anatomical descriptions and taxonomic identifications of new theropod fossil materials from the Cenomanian of the Kem Kem Group. A brief review of theropod occurrences from this geological unit is also provided. All described materials studied here come from the Tafilalt region of south-eastern Morocco, close to the border with neighbouring Algeria, in the Taouz area (see below). The dinosaur remains comprise mainly spinosaurids; however, a carcharodontosaurid specimen is also described.

Geological and depositional settings

The Kem Kem Group or the informal Kem Kem beds is a Cretaceous lithostratigraphic unit that extends along the Algerian–Moroccan border (Fig. 1) on the north-western limit of the Sahara Desert and also westwards to the Atlas Mountains (Sereno *et al.* 1996, Cavin *et al.* 2010, Ibrahim *et al.* 2020b).

This continental geological unit is characterized by a succession of arid to semi-arid sedimentary depositional environments in a fluvial to coastal system (Belvedere *et al.* 2013, Ibrahim *et al.* 2014b). The Kem Kem Group is included within the Hamadian Supergroup or the '*trilogie mésocrétacée*' of Choubert (1948) and this supergroup comprises a single transgressive sequence (Cavin *et al.* 2010, Ibrahim *et al.* 2020b). The Kem Kem Group rests unconformably on the Silurian, Devonian, and Cambrian marine Palaeozoic strata and it is upwards capped by the Late Cenomanian–Turonian carbonate platform or the Akrabou Formation (Choubert 1948, Ferrandini *et al.* 1985, Ibrahim *et al.* 2020b). The Kem Kem Group consists of the two separated lower non-marine units of the Hamadian Supergroup, as recognized by Ibrahim *et al.* (2020b): (i) the older Gara Sbaa Formation and (ii) the overlying Douira Formation.

The Gara Sbaa Formation (Fig. 1) is mainly composed of reddish fine- and medium-grained sandstone layers and other siliciclastic strata with sedimentary traction structures (Ibrahim *et al.* 2020b). This formation often ends in a cemented sandstone that is conformably overlain by the basal bed of red mudstone of the Douira Formation, which is predominantly composed by finer-grained strata that exhibit more diverse lithologies, such as siliciclastic rocks and evaporites (Ibrahim *et al.* 2020b).

The Kem Kem Group has a continental status and has long been proposed to have been formed in a deltaic palaeoenvironment draining northwards towards the Tethys Ocean and secondarily westwards towards the Atlantic Ocean (Defaud and Zellouf 1995, Sereno *et al.* 1996, Cavin *et al.* 2010, Essafraoui *et al.* 2015, Ibrahim *et al.* 2020b). The Gara Sbaa Formation was formed in a large anastomosed fluvial system that eroded the Palaeozoic strata when a prograding deltaic environment was established. In the upper part of the Douira Formation, these deltaic deposits turn into coastal deposits and sabkas, before a marine transgression occurred, where the Akrabou Formation was formed (Guiraud *et al.* 2005, Cavin *et al.* 2010, Ibrahim *et al.* 2020b).

Regarding the age of the Kem Kem Group, Ibrahim *et al.* (2020b) refined the interpretations and proposed an Early-Mid-Cenomanian age (99.0–93.5 Mya), constituting the Gara Sbaa Formation Lower Cenomanian and the Douira Formation Middle Cenomanian geological packages.

MATERIALS AND METHODS

Studied material

The fossils studied and described here consist of eleven isolated and previously unpublished materials housed at the Natural History Museum of London, United Kingdom. The category of each fossil specimen described herein, as well as their respective institutional identification numbers, are in Table 1. With the exception of specimen NHMUK PV R 38358 (unknown locality), all other materials listed in Table 1 and described here are derived from the Tafilalt region in SW Morocco, an area known as

Figure 1. Map of Morocco (south-eastern) and Algeria (western) showing the outcrops of the Kem Kem Group in the Tafilalt region. The Kem Kem Group rock exposures were adapted from Sereno *et al.* (1996) by Smith *et al.* (2023b) and modified here. The star indicates Taouz, the area from which the fossils described here come from.

Table 1. Skeletal materials studied here.

Categories	Material type	Referred specimen
Cranial remains	Rostrum	NHMUK PV R 16420
	Premaxillae	NHMUK PV R 16422
	Premaxilla	NHMUK PV R 16424
	Nasals	NHMUK PV R 16426
	Frontals	NHMUK PV R 16423
Axial skeleton	Cervical vertebra	NHMUK PV R 38358
	Neural arch	NHMUK PV R 16430
	Neural spine	NHMUK PV R 16431
Appendicular skeleton	Ilium	NHMUK PV R 16391
	Ilium	NHMUK PV R 16438
	Ischium	NHMUK PV R 16437
	Femur	NHMUK PV R 16433

Taouz, in the Sahara Desert (Fig. 1). As a consequence of the uncontrolled acquisition of the material by non-palaeontologists, there is no precise information about the stratigraphic position of each specimen, which is common for fossil specimens from this region (McGowan and Dyke 2009).

Furthermore, we provide a detailed redescription and comparisons based on current knowledge of the NHMUK PV R 16420 rostrum that was originally briefly described by Milner (2003), which is also from an unknown location in the Tafilalt region.

Anatomical terms and muscle homologies

Regarding osteological terms, we mainly follow the revised *Nomina Anatomica Veterinaria* (NAV 2017). However, the anterior and posterior anatomical directions were used instead of the cranial and caudal directions, respectively. The nomenclature

and myological homology follow the propositions of Hutchinson (2001a,b), Carrano and Hutchinson (2002), as well as Baumel and Witmer (1993), in the descriptions of some osteological correlates. The few muscular inferences provided here are based on the reconstruction method formalized by Witmer (1995).

Institutional abbreviations

CMP, Mas de la Parreta Quarry, Morella, Spain; FSAC, Faculté des Sciences Aïn Chock, Casablanca, Morocco; MDS, Dinosaur Museum of Savannakhet, Savannakhet, Laos; MN, Museu Nacional/Universidade Federal do Rio de Janeiro, Rio de Janeiro, Brazil; MNHN, Muséum National d'Histoire Naturelle, Paris, France; MNN, Musée National du Niger, Niamey, Niger; MSNM, Museo di Storia Naturale di Milano, Milan, Italy; NHMUK, Natural History Museum, London, United Kingdom; ROM, Royal Ontario Museum, Toronto, Canada; SNSB/BSPG, Bayerische Staatssammlung für Paläontologie und Geologie, Munich, Germany.

RESULTS AND DISCUSSION

Systematic palaeontology

Theropoda Marsh, 1881

Tetanurae Gauthier, 1986

Orionides Carrano *et al.*, 2012

Megalosauroidea Fitzinger, 1843 *sensu* Carrano *et al.*, 2012

Spinosauridae Stromer, 1915

Spinosaurinae Stromer, 1915 *sensu* Sereno *et al.*, 1998

Spinosaurinae gen. et sp. indet.

(Figs 2–12)

Referred specimens

An almost complete rostrum preserving both premaxillae, maxillae, and the anterior portion of the nasals (NHMUK PV R 16420); a paired premaxillae with a fragment of attached maxilla (NHMUK PV R 16422); and a fragment of an isolated right premaxilla (NHMUK PV R 16424); conjoined nasals (NHMUK PV R 16426); a partial skull roof comprising two fused frontals, left prefrontal, and the posterior portion of the left nasal (NHMUK PV R 16423); a mid-dorsal neural arch (NHMUK PV R 16430); a fragmentary mid-dorsal neural spine (NHMUK PV R 16431); two partial ilia (NHMUK PV R 16391 and NHMUK PV R 16438); and a nearly complete left femur (NHMUK PV R 16433).

Morphological description (rostrum)

NHMUK PV R 16420 consists of the paired premaxillae, mainly the anterior body of the right and left maxillae, and the anterior portions of the conjoined nasals (Fig. 2). The anterior end of the snout is damaged and seems to be slightly taphonomically deformed (e.g. Fig. 2C). The rostrum is anteroposteriorly long (Milner 2003), being *c.* 600 mm in length, lateromedially compressed and dorsoventrally rather low (Fig. 2A–C). In lateral view (Fig. 2A–C), the dorsal surface of the rostrum is straight anteriorly, posteriorly becoming concave. The ventral surface is heavily concave anteriorly and straightens posteriorly at the level of the fourth maxillary alveolus [elongate 'S-curve' of Milner (2003)]. The anterior tip of the premaxillae does not project ventral to the maxillary tooth row (Fig. 2A, B). The preserved rostral roof is formed by the premaxillae and the nasals, with the skull roof being narrow mediolaterally. Ventrally the rostrum thickens because the lateral walls of the maxillae are ventrolaterally directed—both the premaxillae and maxillae exhibit a sinusoidal groove (Isasmendi *et al.* 2023), which separates the lateral dentigerous section from the medial part of the rostral bones and creates a secondary palate visible along the entire lateral view (Fig. 2A, B). The external nares are significantly retracted posteriorly, at about 560 mm from the anterior tip of the snout, and they are proportionately small, being located between the eighth and ninth maxillary alveoli (Fig. 2A, B). The premaxilla does not participate in the external nares. Instead, the latter is delimited anteriorly, ventrally, and posteriorly by the maxillae, and dorsally by the nasals (Fig. 2A, B). Although the entire shape of the external naris cannot be determined, the anterior and dorsal margins are relatively straight and the posteroventral margin seems to be concave in shape (Fig. 2A).

Premaxillae

The paired premaxillae of the NHMUK PV R 16420 specimen suggest that the dorsal rim was partially fused, potentially indicating that this individual was nearly a somatically mature animal. In the other specimens, NHMUK PV R 16422 (Fig. 3) and NHMUK PV R 16424 (Fig. 4), no bony fusion can be noticed, suggesting that these were somatically immature individuals. The premaxillary body of the NHMUK PV R 16420 rostrum is *c.* 200 mm in length anteroposteriorly and *c.* 120 mm in height, with a *c.* 90 mm broad premaxillary 'rosette' (*sensu* Charig and Milner 1997). If the posterodorsal process of the premaxilla is considered, this would be *c.* 570 mm long anteroposteriorly (Fig. 2). The premaxillae of NHMUK PV R 16420 contact the nasals posterodorsally and the maxillae posteroventrally (Fig. 2A, B). The anteriormost portion of all the studied premaxillae is damaged and its shape cannot be determined; however, the anterior premaxillary 'rosette' is present, at least partially, in all of them [see Milner (2003) and this work for NHMUK PV R 16420]. Posterior to the 'rosette', the premaxillary body is constricted both dorsoventrally and mediolaterally (Figs 2–4). In lateral view (Fig. 2A, B, H–K), the anteroventral margin of the NHMUK PV R 16420 premaxillae projects anteroventrally—the anterior surface of the premaxillae is convex, straightening dorsally, while the ventral surface is concave throughout its entire length. The lateral wall of the premaxillae is thoroughly rugose and bears several neurovascular foramina that pierce the premaxilla (e.g. Fig. 3E–H). Generally, the foramina are oval to subcircular in shape and exhibit a ventrally oriented shallow groove, which can be straight or parabolic. The ventral foramina form a row that is parallel to the ventral surface of the lateral wall. The dorsal foramina seem to be scattered. Also in lateral view, the alveolar row can be distinguished (see Figs 2–4).

As aforementioned, the external naris is considerably retracted posteriorly (Fig. 2A, B), the typical nasal and subnarial processes of the premaxilla that delimit the external naris dorsally and ventrally, as seen in other theropods, is not present. Nevertheless, two equivalent processes (i.e. the posterodorsal and posteroventral processes of the premaxillae; Fig. 2A, B) are present in the NHMUK PV R 16420 individual, which delimit

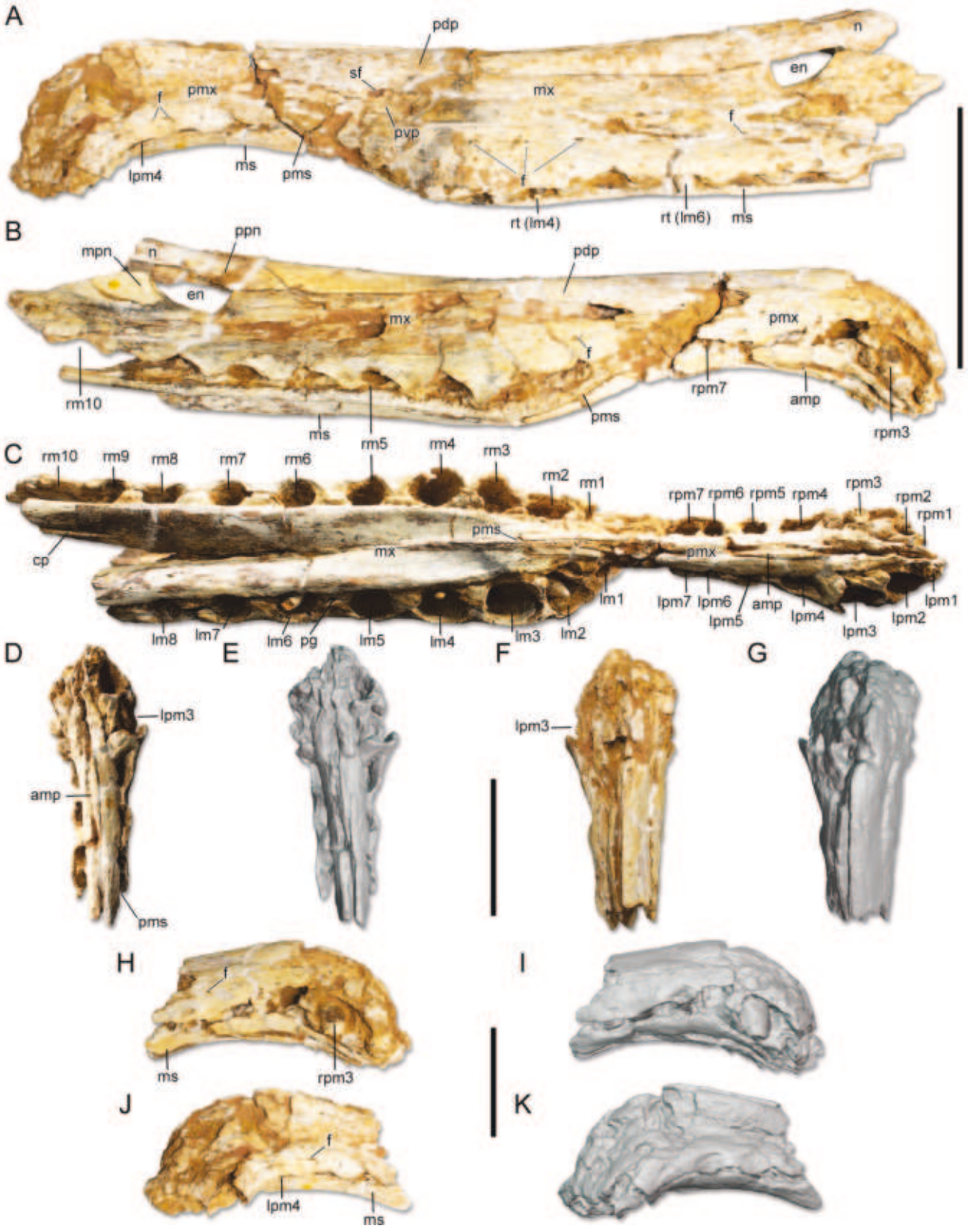

Figure 2. Rostrum of Spinosaurinae indet. NHMUK PV R 16420. Snout in (A) left lateral, (B) right lateral, and (C) ventral views; premaxillae in (D, E) ventral, (F, G) dorsal, (H, I) right lateral, and (J, K) left lateral views. Anatomical abbreviations: amp, anteromedial process; cp, contact with palatine; en, external nares; f, foramen; lm, left maxillary alveolus; lpm, left premaxillary alveolus; mpn, medial process of the nasal; ms, medial shelf; mx, maxillae; n, nasal; pdp, posterodorsal process of the premaxilla; pg, paradental groove; pms, premaxilla–maxilla suture; pmx, premaxillae; ppn, posterodorsal process of the nasal; rm, right maxillary alveolus; rpm, right premaxillary alveolus; rt, replacement tooth; sf, subnarial foramen. Scale bar equals 200 mm (A–C) and 100 mm (D–K).

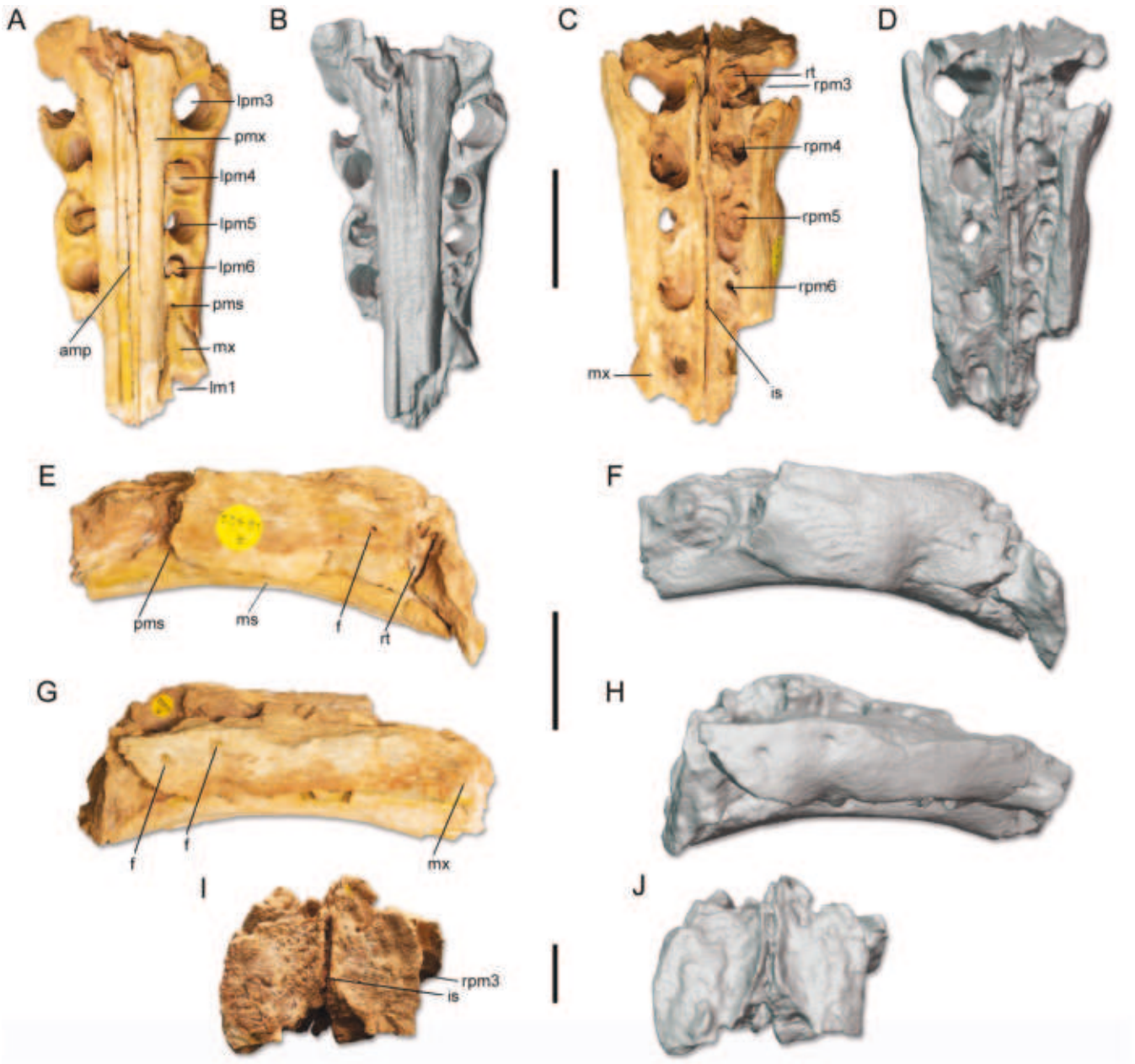

Figure 3. Premaxillae of Spinosaurinae indet. NHMUK PV R 16422. A, B, ventral; C, D, dorsal; E, F, right lateral; G, H, left lateral, and I, J, anterior views. Anatomical abbreviations: amp, anteromedial process; f, foramen; is, intrapremaxillary suture; lpm, left premaxillary alveolus; ms, medial shelf; mx, maxillae; pms, premaxilla–maxilla suture; pmx, premaxillae; rpm, right premaxillary alveolus; rt, replacement tooth. Scale bar equals 50 mm (A–H) and 20 mm (I–J).

the subnarial foramen (better preserved on the left lateral side; Fig. 2A). The posterodorsal process of the premaxillae mainly projects posteriorly, being long and forming the skull roof between its base and the nasals, and gradually tapering posteriorly (Fig. 2A, B). This process is straight and anteriorly horizontal; however, it slightly projects posterodorsally, as seen in lateral view (Fig. 2B). The ventral surface of the posterodorsal process contacts the maxilla ventrally from its base to slightly anterior to the external naris; posteriorly it contacts the nasals. The contact between the premaxillae and nasals has a complex morphology. In dorsal view, the premaxillae and nasals contact each other dorsally and interlock via a 'peg-like' process that extends from each premaxillae penetrating the nasals, giving it a 'W-shape' morphology at the contact region. The posteroventral process of the premaxillae is considerably less-developed; however, it is taphonomically damaged (mainly on the right side; Fig. 2B). This tapering process is posteriorly directed and laterally overlaps the maxillae. The bases of the posterodorsal and posteroventral processes are separated by the subnarial foramen (Fig. 2A). In ventral view, each premaxilla (i.e. NHMUK PV R 16420, NHMUK PV R 16422, and NHMUK PV R 16424) exhibits a medially placed robust bone element, forming a convex secondary palate. That secondary palate is also visible in lateral view due to the lateral walls of the premaxillae, which do not project ventrally (Figs 2–4). These elements are divided from the lateral dentigerous portion of the premaxillae by a sinusoidal

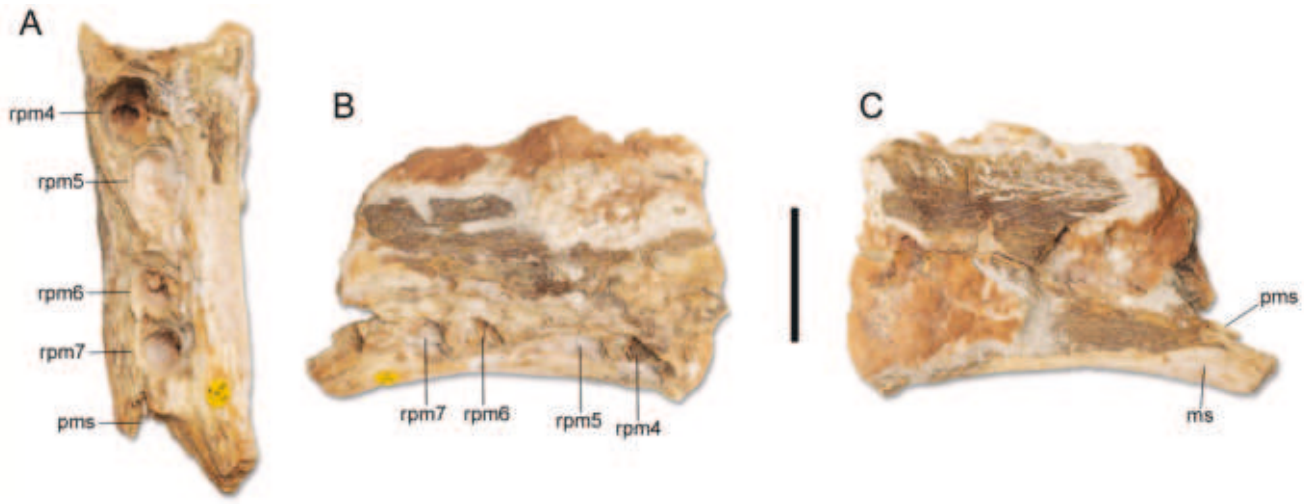

Figure 4. Fragmentary premaxilla of Spinosaurinae indet. NHMUK PV R 16424. A, ventral; B, right lateral; and C, medial views. Anatomical abbreviations: ms, medial shelf; pms, premaxilla–maxilla suture; rpm, right premaxillary alveolus. Scale bar equals 50 mm.

groove. The robust bone elements meet anteromedially at the level of the second and third premaxillary alveoli (e.g. Fig. 2C, D). This medial contact consists of the interdigitation of both elements, whereas they are posteriorly separated by a gap and, more posteriorly, by the anteromedial processes of the maxillae (Milner 2003).

The dentigerous portions of the premaxillae are concave (Figs 2H–J, 3E–H, 4B, C). Each of the NHMUK PV R 16420 premaxillae bear seven alveoli, which are subcircular in shape (Milner 2003, Lacerda *et al.* 2022). The anteriormost alveolus (premaxillary alveolus 1; pm1) is small, and the second (pm2) and third ones (pm3) are considerably larger, being the largest alveoli of the premaxillary row; towards the rear of the skull, the premaxillary alveoli decrease in size. The fourth (pm4) and fifth alveoli (pm5) are separated from their anterior and posterior ones by a diastema; and the sixth (pm6) and seventh alveoli (pm7) are 'coupled' in the studied premaxillae (Figs 2C, D, 3A, B, 4B, C), similar to other spinosaurines (Lacerda *et al.* 2022). Between the last premaxillary alveolus (pm6 or pm7) and the first maxillary tooth (mx1), another diastema is present. In NHMUK PV R 16422 and NHMUK PV R 16424, the posterior four alveoli are preserved, which gradually decrease in size posteriorly (Figs 3A, B, 4B, C). If the pattern observed in the spinosaurine specimens, such as NHMUK PV R 16420, MNHN SAM 124, and MSNM V4047, is considered (Taquet and Russell 1998, Milner 2003, Dal Sasso *et al.* 2005, Lacerda *et al.* 2022), the NHMUK PV R 16422 individual would bear six premaxillary teeth and thus the preserved alveoli are interpreted as pertaining to pm3 to pm6 (Fig. 3A–D). On the other hand, the specimen NHMUK PV R 16424 would exhibit seven alveoli on its right premaxilla and the preserved ones would correspond to pm4 to pm7 (Fig. 4). Alveolar metrics are in Table 2.

In the left premaxilla of NHMUK PV R 16422, lpm3 is separated from the rest of the premaxillary alveoli by a diastema (Fig. 3A, B). In the right premaxilla of NHMUK PV R 16422 and the right premaxilla NHMUK PV R 16424 (Fig. 4), the two anterior preserved alveoli (pm3–4 of NHMUK PV R 16422 and pm4–5 of NHMUK PV R 16424), as well as the two most posterior alveoli (pm5–6 of NHMUK PV R 16422 and pm6–7 of NHMUK PV R 16420), are paired and separated from each other by a diastema (Figs 2–4). Another diastema is present between the last alveolus of the premaxilla (pm6/7) and the maxilla (m1). In the regions of the premaxillae where the diastemata are located, the lateral walls of the premaxillae have ventrally located concavities (Fig. 2A, B), where the laterocumbent teeth of the dentary would probably have inserted, as indicated by Dal Sasso *et al.* (2005). The overall outline of the preserved alveoli is subcircular in all three specimens (Figs 2–4).

Both NHMUK PV R 16420 and NHMUK PV R 16422 still retain some teeth preserved *in situ*. In NHMUK PV R 16420, these are present in the lpm1 on the left side, and the rpm3 in the right premaxilla, and comprise the bases and roots of the teeth (Fig. 2C–H). In the NHMUK PV R 16422 specimen, teeth are preserved in the alveoli lpm4 and lpm6 of the left premaxilla and rpm3 and rpm5 of the right premaxilla (Fig. 3). However, these teeth are not completely erupted, being replacement teeth (e.g. rt in Fig. 3E). The general dentition is conidont, being not distally recurved, with a centrally located apex, and laterocumbent (*sensu* Hendrickx *et al.* 2019). The basal cross-section of the teeth is subcircular and lenticular in the middle of the crown. The mesial and distal carinae are not denticulated and their basal portion reaches the cervix. The mesial carinae of the teeth of NHMUK PV R 16422 are oriented mesiolingually and the distal carinae are oriented distolabially, mainly based on rpm5 and lpm6 (Fig. 3A, B). The enamel texture of the crowns is veined/anastomosed (*sensu* Hendrickx *et al.* 2015). The largest tooth in NHMUK PV R 16420 (rpm3) exhibits flutes, at least on the labial surface of the crown. However, the teeth of NHMUK PV R 16422 are devoid of flutes, with the labial and lingual surfaces of the crown being smooth.

Maxillae

The NHMUK PV R 16422 specimen only preserves the anteromedial processes of a maxilla and the most anteroventral point of the left maxilla, including the mesial border of the left maxillary alveolus 1 (Fig. 3A–D). Therefore, our description focuses mainly on the well-preserved maxillae of NHMUK PV R 16420.

Table 2. Measurements of the premaxillary alveoli of Spinosaurinae specimens NHMUK PV R 16420, NHMUK PV R 16422, and NHMUK PV R 16424.

NHMUK PV R 16420	**pm1**	**pm2**	**pm3**	**pm4**	**pm5**	**pm6**	**pm7**
Anteroposterior length of the left premaxilla	14 mm	?	41 mm	24 mm	14 mm	?	?
Lateromedial width of the left premaxilla	10 mm	20 mm	?	18 mm	10 mm	?	?
Anteroposterior length of the right premaxilla	?	?	47 mm	29 mm	21 mm	20 mm	?
Lateromedial width of the right premaxilla	8 mm	?	?	14 mm	16 mm	16 mm	?
NHMUK PV R 16422	**pm1**	**pm2**	**pm3**	**pm4**	**pm5**	**pm6**	--
Anteroposterior length of the left premaxilla	?	?	20 mm	16 mm	17 mm	9 mm	--
Lateromedial width of the left premaxilla	?	?	25 mm	16 mm	13 mm	10 mm	--
Anteroposterior length of the right premaxilla	?	?	23 mm	16 mm	14 mm	16 mm	--
Lateromedial width of the right premaxilla	?	?	?	15 mm	14 mm	15 mm	--
NHMUK PV R 16424	**pm1**	**pm2**	**pm3**	**pm4**	**pm5**	**pm6**	**pm7**
Anteroposterior length of the right premaxilla	?	?	?	29 mm	20 mm	18 mm	16 mm
Lateromedial width of the right premaxilla	?	?	?	24 mm	21 mm	18 mm	17 mm

Each maxilla of the NHMUK PV R 16420 snout mainly preserves the anterior portion of the maxillary body and the base of the ascending process of the maxilla (Fig. 3), thus, there is no sign of the jugal processes. The maxilla is elongated (Milner 2003), with a preserved length of *c.* 420 mm. The anterior body of the maxilla is continuous in depth (*c.* 100 mm), becoming deeper at the level of the ascending process (Fig. 2A, B). The anterior process of the maxilla is hypertrophied and contacts the premaxilla anteriorly in ventral view (Fig. 2C). The anteroventral contact between the premaxilla and the maxilla is not preserved, but just adjacent to the subnarial foramen, the posteroventral process of the premaxilla interlocks with the maxilla (Milner 2003). Posterodorsally, the premaxillary–maxillary contact becomes more horizontal and straighter, slightly curving dorsally anterior to the premaxillary–nasal contact (Fig. 2A, B). The intermaxillary suture extends from the most anterior portion of the maxillae to the region of the eighth maxillary alveoli (m8) (Milner 2003). Anteriorly, the intermaxillary suture, between alveoli m1 and m2, presents an interdigitated pattern (Fig. 2C). In lateral view, the ventral margin of the maxilla faces anteroventrally and subsequently this margin gradually faces ventrally proximally, with a medial shelf being evident in lateral view (Fig. 2B, C). In ventral view, the maxilla tapers anteriorly, widening posteriorly. The maxilla is widest at the level of the m4, narrowing slightly posteriorly and widening towards the back of the skull. Therefore, in ventral view, the lateral wall is 'S-shaped' and directed lateroventrally (Fig. 2C).

The lateral surface of the maxilla is smooth, being perforated by numerous neurovascular foramina with a subcircular to oval outline (Fig. 2A). Basally, these foramina are arranged in an anteroposteriorly oriented row that is parallel to the ventral margin of the lateral wall of the maxilla and interpreted as maxillary alveolar foramina. In addition to these, other scattered foramina are present on the lateral wall of the maxilla and are interpreted as median maxillary foramina. In ventral view, the lateral wall of the maxilla is sinusoidal, being convex due to the projection of the lateral wall along the alveoli, and concave between the alveoli (Fig. 2C).

The maxillae bound the anterior, ventral, and posterior edges of the external nares. In NHMUK PV R 16420, the external naris is retracted posteriorly and reduced, being positioned between alveoli m7 and m9 (Fig. 2A, B). Adjacent to the external naris, the maxilla exhibits a fossa that deepens posterodorsally so that a thin bone lamina (or nasal process—Dal Sasso *et al.* 2005) projects dorsally into the ventral margin of the external naris. Posteriorly, the base of the ascending process of the maxilla is present, which is overlapped by the maxillary process of the nasal (Fig. 2B). However, the ascending process is poorly preserved.

In ventral view, the anteromedial processes are basally located in the maxillae and project anteriorly from the level of alveoli m3 reaching the pm4. The anteromedial processes medially divide the conjoined premaxillae ventrally, so that the premaxillary–maxillary contact is 'peg-like' or 'finger-like' (Milner 2003) in ventral view (Fig. 2C). Both processes contact each other medially almost throughout their entire extent, but they diverge at their anteriormost end in the premaxilla.

The medial shelf in NHMUK PV R 16420 is located on the medial surface of the maxilla and ventrally displaced, being a smooth cylinder-like bony bar (Fig. 2A–C). The medial shelf projects more ventrally than the lateral wall of the maxilla along its entire extension (Fig. 2A, B). The ventromedial surface of the medial shelf is quite flattened anteriorly and this surface becomes rounded posteriorly. Both medial shelves contact each other from the m3 to the m8 alveoli (Milner 2003), forming a secondary palate visible in lateral view (Fig. 2A–C). This contact gradually increases posteriorly and from m8 towards the rear of the skull, the maxillae would come into contact with the nasals in ventral view. In the same view, both maxillae present an anteroposteriorly oriented groove at the posteriormost end that is interpreted as the contact for the palatine (Fig. 2C). The medial shelf dorsomedially limits the interdental plates, which are somewhat rough and oriented ventrolaterally. These are more dorsoventrally oriented anteriorly and become more horizontal posteriorly (Fig. 2C). Regarding their shape, these are anteriorly 'V-shaped' and become subquadrangular from m5 onwards.

Furthermore, in ventral view, the interdental plates with the continuous paradental bone (*sensu* Currie 1987) are 'hourglass-shaped' (Fig. 2C). The interdental plates are fused together to form an interdental wall. The paradental groove (nutrient groove *sensu* Hendrickx and Mateus 2014) is located between the interdental wall and the medial shelf, dividing the lateral and medial half of the maxilla (Fig. 2C). The paradental groove is sinusoidal in ventral view due to its adjustment with the maxillary alveoli (Isasmendi *et al.* 2023).

Because the NHMUK PV R 16420 maxillae are not posteriorly complete, the total number of maxillary alveoli cannot be accurately determined. Nevertheless, 10 subcircular-shaped alveoli are preserved in the right maxilla and eight in the left (Fig. 2C). All the alveoli measurements are provided in Table 3.

The alveoli increase in size from m1 to m4 and then gradually become smaller thereafter (Fig. 2C; Table 3). The three anterior alveoli are oriented anteroventrally, and from the fourth toward the rear of the skull, the alveoli are oriented slightly ventrolaterally rather than ventrally. Hence, an inflection point can be noticed between the alveoli m3 and m4. The anterior alveoli are closer packed (i.e. m1 to m4) and become more spaced posteriorly in the skull, so that more posteriorly located alveoli have the anteroposterior distance between adjacent alveoli similar to the anteroposterior length of the alveoli themselves (Fig. 2C).

Most of the maxillary alveoli of NHMUK PV R 16420 do not have teeth *in situ*; however, they are present in alveoli lm2, lm4, and lm6 (Fig. 2A, C). Since the preserved teeth are not fully erupted (e.g. lm4 and lm6 in Fig. 2A) and are located lingually in the alveoli, these are interpreted as replacement teeth. Similar to the premaxillary dentition, the teeth of the left maxilla have a conidont morphology, the crowns are straight with a centrally located apex. The enamel texture is veined/anastomosed and several flutes are present, at least on the lingual surface of the crown. The basal cross-section of the teeth appears to be subcircular and lenticular in the middle of the crown. The mesial and distal carinae are present and do not have denticles/serrations. Notably, the lm2 tooth is procumbent, while the other two, lm4 and lm6, are laterocumbent (Fig. 2C).

Nasals

Only the anterior portion of the conjoined nasals is preserved in the NHMUK PV R 16420 specimen. Additionally, a posterior portion of an isolated conjoined nasal (NHMUK PV R 16426) is also presented (Fig. 5). The preserved portion of the nasals contacts the premaxilla anteriorly and the maxilla anteroventrally, so that the nasals form part of the skull roof, slightly anterior to the external nares towards the posterior part of the skull. Furthermore, the maxillary and premaxillary processes of the nasals are projected laterally on the rostrum, participating in the lateral wall of the skull (Fig. 2A, B).

The premaxillary and maxillary processes of the nasal bifurcate laterally anteriorly at the posterior margin of the external nares. The premaxillary process of the nasals delimits the straight dorsal margin of the external nares (Fig. 2A, B). The maxillary processes may have delimited the posterior margin of the external nares, but this area is not preserved. The maxillary process of the external nares does not bound its posteroventral margin.

The premaxillary processes diverge from the dorsal margin and extend on to the lateral surface of the skull above the external nares, more anteriorly than the external nares and overlapping the maxilla laterally. The premaxillary process is projected anteriorly and tapers anteriorly. In lateral view, this is almost horizontal, with its dorsal margin sloping anteroventrally and the ventral margin nearly horizontal (Fig. 2A, B).

The maxillary process is projected anteroventrally, tapers anteroventrally, and contacts the maxilla laterally. The ventral margin of this process overlaps the maxilla and, posteriorly, this overlap gradually decreases, as the ventral margin of the nasal process ascends posteriorly (Fig. 2A, B). In posterior view, the nasal shaft has an arched morphology, with a convex

Table 3. Measurements of the maxillary alveoli of Spinosaurinae specimen NHMUK PV R 16420.

NHMUK PV R 16420	m1	m2	m3	m4	m5	m6	m7	m8	m9	m10
Anteroposterior length of the left maxilla	13 mm	26 mm	37 mm	36 mm	27 mm	27 mm	23 mm	22 mm	?	?
Lateromedial width of the left maxilla	9 mm	?	31 mm	25 mm	20 mm	20 mm	18 mm	17 mm	?	?
Anteroposterior length of the right maxilla	?	30 mm	32 mm	36 mm	26 mm	25 mm	25 mm	24 mm	?	?
Lateromedial width of the right maxilla	?	17 mm	27 mm	37 mm	20 mm	20 mm	19 mm	15 mm	?	?

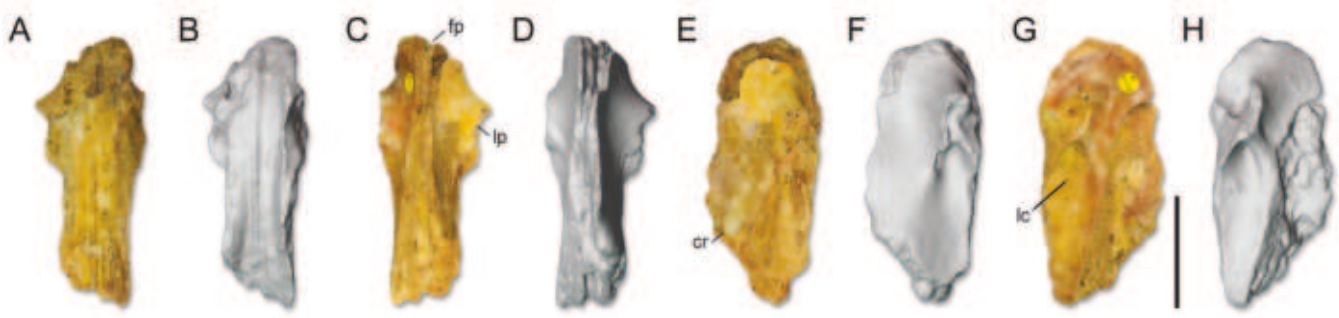

Figure 5. Isolated frontals of Spinosaurinae indet. NHMUK PV R 16426. A, B, dorsal; C, D, ventral; E, F, left lateral; and G, H, right lateral views. Anatomical abbreviations: cr, crest; fp, frontal process; lc, lateral concavity; lp, lacrimal process. Scale bar equals 50 mm.

dorsal margin and a concave ventral surface. The suture line of the nasals is still visible on the preserved portion and no sagittal crest is present on the dorsal surface.

The posterior portion of the conjoined nasals (NHMUK PV R 16426) is raised into a sagittal crest giving it an inverted-'V shape', which is more intact on the left nasal (Fig. 5A–D). The lateral surface of this crest is smooth, but inside it is pneumatic, as seen in the right nasal, which is abraded and has large foramina in its upper section (Fig. 5G, H). The dorsal edge of the crest has a crenulated profile when viewed from the side. The junction with the lacrimal has a 'wing-like' shape when viewed from above, featuring a deep concavity at the front and a posteroventral concavity at the back (Fig. 5E–H). The posterior portion of the nasal, where it contacts the frontals, is convex when viewed from the side, though the very end of this portion is abraded. In posterior view, this section has a longitudinal groove, with a chambered structure, indicating it was highly pneumatized. The internal (ventral) surface of the nasals is slightly concave and divided by a low sagittal ridge running from front to back. This internal area is mostly smooth, except for a few small foramina and parallel striations. The conjoined nasals narrow slightly at the midpoint of the preserved bones, widen towards the posterior end where they meet the lacrimal, and then narrow again at the very back where they meet the frontal (Fig. 5A–D). However, this last section is broken, missing the tip of the bone.

Morphological comparisons

As the skull of spinosaurids is highly derived and specialized, many synapomorphies can be found within their cranium. Owing to this, specimens NHMUK PV R 16420, NHMUK PV R 16422, and NHMUK PV R 16424 share many derived traits with Spinosauridae, as follows.

The premaxillae of the specimens studied here are hypertrophied and fused (except the poorly preserved NHMUK PV R 16424), with a concave ventral margin in lateral view, posteriorly tapered, and displaying more than five alveoli as in Spinosauridae (Carrano *et al.* 2012, Barker *et al.* 2021, Lacerda *et al.* 2022, Schade *et al.* 2023). Furthermore, the premaxillary–maxillary articulation is interlocked as in Spinosauridae, rather than flat as in the other early-diverging theropods; additionally, the external nares are posteriorly retracted (Sereno *et al.* 1998, Taquet and Russell 1998, Dal Sasso *et al.* 2005, Sales and Schultz 2017, Rauhut and Pol 2019, Barker *et al.* 2021, Schade *et al.* 2023).

Regarding the maxillae, NHMUK PV R 16420 shares the following anatomical features with Spinosauridae: (i) the hypertrophied anterior process of the maxillae; (ii) a plate-shaped anteromedial process of the maxillae, long and projecting far anteriorly; (iii) a proportionally anteroposterior and mediolaterally large, and cylinder-shaped medial shelf; (iv) the sinusoidal lateral wall of the maxilla in ventral view; (v) the size pattern of the alveoli that increases from m1 to m4 and then gradually decreases towards the rear of the skull; (vi) anterior alveoli that are angled anteriorly due to a convex anterior maxillary border; (vii) procumbent anterior maxillary teeth; (viii) conidont dentition; and (ix) veined/anastomosed enamel texture of the crowns (Charig and Milner 1997, Sereno *et al.* 1998, Taquet and Russell 1998, Sues *et al.* 2002, Dal Sasso *et al.* 2005, Canudo *et al.* 2008, Benson 2010, Kellner *et al.* 2011, Carrano *et al.* 2012, Hendrickx and Mateus 2014, Hendrickx *et al.* 2015, 2019, Alonso *et al.* 2017, 2018, Sales and Schultz 2017, Rauhut and Pol 2019, Isasmendi *et al.* 2023, Schade *et al.* 2023, Souza *et al.* 2023). Furthermore, the nasals are also at least partially fused in NHMUK PV R 16420, as observed in Spinosauridae (Carrano *et al.* 2012).

Within Spinosauridae, the premaxillary alveoli paired with the presence of diastemata of the specimens described here, as well as the small pm1 tooth/alveolus compared to the other premaxillary teeth/alveoli, are also features shared with Spinosaurinae species, and the latter feature is also present in the baryonychine *Riparovenator* (Dal Sasso *et al.* 2005, Carrano *et al.* 2012, Barker *et al.* 2021, Lacerda *et al.* 2022). Furthermore, the alveolar row is interrupted by the premaxillary–maxillary contact in NHMUK PV R 16420, a feature recovered as a synapomorphy of Spinosaurinae by Barker *et al.* (2021).

Other features found in the maxillae of NHMUK PV R 16420 snout that are worth highlighting are: (i) lateral wall not projected too far ventrally, so that the lateral maxillary alveoli are visible in lateral view; (ii) conidont teeth with a very subcircular cross-sectional base, without denticles in the distal and mesial carinae; (iii) laterocumbent lateral teeth; and (iv) presence of diastema in the maxillary teeth (Charig and Milner 1997, Carrano *et al.* 2012, Hendrickx *et al.* 2015, 2019, Alonso and Canudo 2016). Moreover, the medial shelves of the maxillae in NHMUK PV R 16420 are strongly medially directed, the paradental groove is sinusoidal in ventral view, and the external nares are strongly retracted posteriorly as in other North African spinosaurines (e.g. MNHN SAM 124 and MSNM V4047) (Dal Sasso *et al.* 2005, Sales and Schultz 2017, Barker *et al.* 2021, Isasmendi *et al.* 2023, Souza *et al.* 2023).

In NHMUK PV R 16420, the maxillae delimit the external nares ventrally and posteroventrally, also as in MSNM V4047 and *Irritator* (Dal Sasso *et al.* 2005, Schade *et al.* 2023). However, in *Irritator* the narial margin is comparatively more anteriorly placed (Sales and Schultz 2017, Isasmendi *et al.* 2023) and the latter has a straighter paradental groove. The sinusoidal paradental groove is also present in *Oxalaia*, but the medial platform is not as medially projected (Isasmendi *et al.* 2023). Therefore, based on the above, the NHMUK PV R 16420, NHMUK PV R 16422, and NHMUK PV R 16424 specimens can be safely assigned to Spinosauridae, and furthermore, based on the stricter comparisons they can be assigned to Spinosaurinae.

Lakin and Longrich (2019) compared the NHMUK PV R 16420 snout [NHMUK 16665 in Lakin and Longrich (2019)] with the MSNM V4047 rostrum and proposed different morphotypes based on some morphological differences in the premaxilla, maxilla, and morphology of external nares, attributing these differences to ontogenetic changes, sexual dimorphism, or distinct taxa. The possibility that they belonged to two different taxa was later ruled out by (Smyth *et al.* 2020b), who assigned the NHMUK PV R 16420 and MSNM V4047 to the same taxon. Lacerda *et al.* (2022) also noted that in the premaxillae of Spinosaurinae specimens from North Africa, there are specific differences such as the degree of constriction of the posterior region of the premaxilla and the degree of expansion of the anterodorsal edge of the premaxilla, as well as the size and location of alveoli pm3 and pm4, which may be due to taphonomic alterations. Based on the reassessment of NHMUK PV R 16420 provided here, we highlight that the only significant difference between the two rostra is the number of premaxillary

teeth and the pattern of the intramaxillary suture anteriorly. Six premaxillary alveoli are present in MSNM V4047 and seven in NHMUK PV R 16420 (Dal Sasso *et al.* 2005), as in MNHN SAM 124 (Taquet and Russell 1998). However, this feature seems to have no systematic significance, because the right premaxilla of *Baryonyx* has six alveoli, whereas the left has seven (Charig and Milner 1997, Hendrickx *et al.* 2016, Lacerda *et al.* 2022).

In ventral view, at the level of alveoli m3 and m4, the maxillae of NHMUK PV R 16420 have a curvature similar to that observed in MSNM V4047, and differing from MNHN SAM 124, in which the curvature is not as pronounced. Furthermore, the dorsoventral constriction of the posterior portion of the premaxillae of NHMUK PV R 16420 is more similar to that observed in MSNM V4047 and less pronounced than the constriction of the snout of MNHN SAM 124 (thus, MNHN SAM 124 is distant in the premaxilla morphospace from NHMUK PV R 16420 and MSNM V4047 based on analysis in lateral view—Lacerda *et al.* 2022). Besides that, the anteriormost alveolar foramina are much smaller in NHMUK PV R 16420 than in MNHN SAM 124, and similar to those found in MSNM V4047. Therefore, due to these similarities, NHMUK PV R 16420 is considered the same taxon as MSNM V4047. NHMUK PV R 16420 was previously assigned to cf. *Spinosaurus aegyptiacus* by Milner (2003) and MSNM V4047 assigned to *Spinosaurus* cf. *aegyptiacus* by Dal Sasso *et al.* (2005). Other studies (e.g. Ibrahim *et al.* 2014a, Smyth *et al.* 2020b) considered NHMUK PV R 16420, MSNM V4047, and MNHN SAM 124 to belong to *Spinosaurus aegyptiacus*. Nevertheless, as previous work has suggested (e.g. Evers *et al.* 2015, Lacerda *et al.* 2022), because the holotype of *Spinosaurus aegyptiacus* lacks these elements for direct comparison and correlation, here we consider NHMUK PV R 16420, NHMUK PV R 16422, and NHMUK PV R 16424 as indeterminate Spinosaurinae.

Posterior portions of spinosaurid nasals are rarely preserved, with only a few species offering points of comparison. The specimen NHMUK PV R 16426 bears resemblance to the spinosaurid nasal UCPC-2 (Dal Sasso *et al.* 2005), although the latter specimen is located more anteriorly in the snout compared to the former one. The lateral profile of the sagittal crest in NHMUK PV R 16426 is similar to those of UCPC-2 and *Baryonyx*, featuring a crenulated lateral profile (Charig and Milner 1997, Dal Sasso *et al.* 2005). However, NHMUK PV R 16426 lacks the longitudinal wrinkles seen in UCPC-2, which are also absent in *Baryonyx*, probably due to its more posterior position in the skull. The high degree of pneumatization in the crest of NHMUK PV R 16426 is also observed in UCPC-2 (Dal Sasso *et al.* 2005), in contrast to the solid nasal crest of *Irritator* (Schade *et al.* 2023), and probably in *Baryonyx* and *Riparovenator*. When viewed from underneath, NHMUK PV R 16426 is broader than the nasal of *Baryonyx*, which narrows towards the front, giving it an 'arrow-like' shape (Charig and Milner 1997). Despite its incompleteness, NHMUK PV R 16426 shows a convex articulation with the frontals, while in *Riparovenator*, the lateral profile of the nasals has a concave shape, and in *Baryonyx*, it is straight (Barker *et al.* 2021).

Morphological description (skull roof)

The specimen NHMUK PV R 16423 is a partial skull roof comprising two frontals, the left prefrontal, and the posterior portion of the left nasal (Fig. 6). The frontals are strongly fused without any signal of suture, measuring 140 mm across the postorbital processes and 160 mm long giving it a width/length ratio of *c.* 87%, being slightly longer than wide. The frontals taper anteriorly, and the width across the contact with the prefrontals is almost 50% of the width at the postorbital processes (Fig. 6A–D). The medial keel is well projected dorsally in the posteriormost portion of the frontals (for contact with parietal) and is flat and wide, dividing the frontals in two deep lateral trapezoidal fossae at middle-length (Fig. 6A, B). In the posteriormost portion of the frontals, the medial keel is tripartite with flat lateral edges and projected 60° through the postorbital processes disappearing laterally. The medial keel follows the concavity of the lateral fossae and rises again in the middle of the frontals where it becomes tripartite again and high for articulation with the nasals (Fig. 6). The posterior edge of the frontals is straight in dorsal view, suggesting a straight profile for the supratemporal fossa that is shallow in posterior view.

The contacts for the postorbitals are 'wing-like' shaped and bipartite, with two large foramina in the anterior portion of each process in dorsal view. The right process is more vascularized than the left, especially in the posterior portion of the process. The dorsal surface of the processes is flat laterally to the lateral edge of the medial keel and concave in the anteriormost portion (Fig. 6). In lateral view, the postorbital contact is dorsoventrally elongated and deeply excavated. The nasal contact extends more than 50% of the frontal length and narrows anteriorly from the level of the posterior prefrontal contact (Fig. 6). It is bifurcated in the anteriormost portion and bears small foramina, longitudinal striae, and a keel in the midline between the frontals, originating from the medial keel in dorsal view (Fig. 6A, B).

The frontals are arched at 40° in lateral view (Fig. 6), making the orbit elevated in the articulated skull. The dorsal orbital margin is circular, with the frontal forming a large part of the orbit. The orbit has a trapezoidal outline in ventral view, with the posterior facet wider than the anterior (Fig. 6C, D).

Most of the ventral bone surface is smooth. A well-defined ridge of the medial orbitonasal region of the lacrimal/prefrontal complex projects posteriorly to form the paired *cristae cranii* (Fig. 6C, D) that border the *sulcus olfactorius* (Fig. 6). Both ridges taper posteriorly, narrowing the sulcus in the middle of the orbit, and widen again to define the lateral border of the cerebral fossae—which are elongated anteroposteriorly and divided by a short, rough septum (Fig. 6C–H). Anterior to this septum, the surface of the bone is crenulated, bearing several small foramina. The contacts of the laterosphenoid are well projected ventrally. They are 'pillar-like' shaped and the ventral surface is very rough and concave (Fig. 6).

The prefrontal has a large contribution to the margin of the orbit, being visible in lateral view (Fig. 6). The contact between the other bones is rough, well-marked with several foramina (suggesting that the specimen was not a mature individual). In the dorsal portion, the prefrontal has a rough crest forming a cornual process in the form of a protrusion that rises from a concave surface (Fig. 6). The posterior process contacts the frontal by a peg-and-socket suture in lateral view, while in ventral view the suture between the bones is tightly interdigitating. Ventrally, the ventral border of the anteroventral process is confluent with the *crista cranii* of the frontals. The anterior process extends more

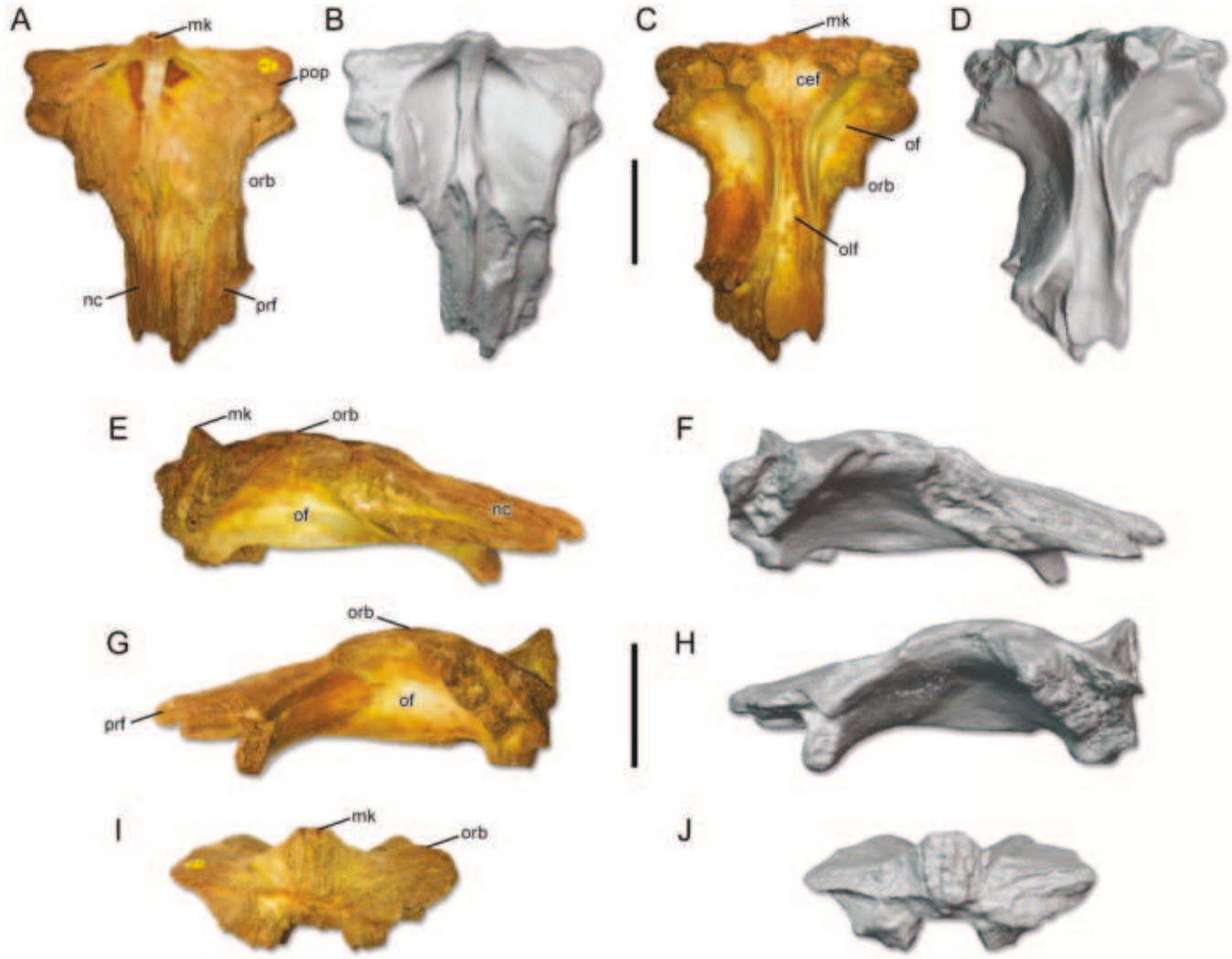

Figure 6. Skull roof of Spinosaurinae indet. NHMUK PV R 16423. A, B, dorsal, C, D, ventral; E, F, right lateral; G, H, left lateral; and I, J, posterior views. Anatomical abbreviations: cef, cerebral fossa; mk, medial keel; nc, nasal contact; of, orbital fossa; olf, olfactory bulbs; orb, orbit; pop, postorbital process; prf, prefrontal. Scale bar equals 50 mm.

anteriorly than the anteroventral process, giving the prefrontal a slight 'T-shape' in lateral view (Fig. 6). The anteroventral process is smaller than the anterior and posterior ones, and inclined almost 45° relative to the roof of the skull.

Morphological comparisons

The frontals of the specimen NHMUK PV R 16423 share the following features with Spinosauridae: (i) participation of the frontals in the orbits; (ii) nasals extending posteriorly over the frontals; (iii) elevated orbital margins; (iv) presence of a well-developed medial keel on the dorsal surfaces of the frontals indicating a well-developed parietal crest; and (v) ventrally deflected rostrum (Arden *et al.* 2019).

However, the participation of the frontal in the orbit varies within Spinosauridae, being absent in *Ceratosuchops* and to a lesser extent in *Riparovenator* (Barker *et al.* 2021), as well as *Baryonyx* and *Suchomimus* (i.e. Baryonychinae). In Spinosaurinae, the frontals are more conspicuous and curved in lateral view (e.g. Arden *et al.* 2019). The frontal excluded from the orbital margin due to the lacrimal/postorbital contact is observed in carcharodontosaurids (e.g. *Meraxes*—Canale *et al.* 2022, *Eocarcharia* and *Carcharodontosaurus*—Sereno and Brusatte 2008), and abelisaurids (e.g. *Majungasaurus*—Sampson and Witmer 2007 and *Carnotaurus*, Cerroni *et al.* 2021), the other two large-bodied theropod groups that are also found in the Kem Kem Group (e.g. Ibrahim *et al.* 2020b).

The overall morphology of NHMUK PV R 16423 resembles those of FSAC-KK-3209, FSAC-KK-3210 ('Morphotype A'), and FSAC-KK-7715 ('Morphotype B') of Arden *et al.* (2019). These specimens were initially proposed as cf. *Spinosaurus aegyptiacus* ('Morph A') and ?*Sigilmassasaurus brevicollis* ('Morph B') based on different proportions. 'Morph B' is shorter and wider, with weaker concave orbital margins, less concave orbital edges, a more deeply excavated postorbital process, a higher sagittal crest, and a wider overlapping contact of the frontals with the prefrontals (Arden *et al.* 2019). Later, Ibrahim *et al.* (2020b:160) commented that Arden *et al* (2019) 'Morph A' resembles the morphology of marine crocodyliforms,

considering the condition of the posterior distance of the braincase in relation to the frontals; however, no detailed morphological redescription/comparison was provided, therefore, we consider here the spinosaurid association of the 'Morph A' braincase provided by Arden *et al.* (2019).

The specimen studied here, NHMUK PV R 16423, has the anterior portion of the frontal tapering to come into contact with the nasals, as in 'Morph A' of Arden *et al.* (2019). NHMUK PV R 16423 is more similar to FSAC-KK-3209, which has the contact for the nasals occupying around 50% of the total frontal length. Also, it resembles 'Morph A' by having a similar curvature and dorsal projection of the orbit in lateral view. Conversely, the general proportion is more similar to 'Morph B' having a width/length ratio of *c.* 87% in NHMUK PV R 16423, compared to the *c.* 93% of 'Morph B' (Arden *et al.* 2019). NHMUK PV R 16423 also shares with 'Morph B' a deep-notched postorbital process, a broad overlapping contact between the frontal and prefrontal, and a high sagittal crest. These features of NHMUK PV R 16423 overlap with the morphology of both morphotypes from Arden *et al.* (2019), which may reinforce the suggestion of Smyth *et al.* (2020b) that the morphotypes represent variations (individual, ontogenetic, or sexual) within a unique species.

In ventral view, NHMUK PV R 16423 presents a closed interfrontal suture, differing from those of *Ceratosuchops*, *Riparovenator* (Barker *et al.* 2021), and possibly FSAC-KK-3209, as well as FSAC-KK-7715 (Figs 2B and 3B respectively—Arden *et al.* 2019). In NHMUK PV R 16423 and 'Morphs A and B' (Arden *et al.* 2019), the nasal overlaps the frontal contact, a different condition observed in *Irritator* (Schade *et al.* 2023), *Ceratosuchops*, and *Riparovenator* (Barker *et al.* 2021). Besides that, in NHMUK PV R 16423 and 'Morphs A and B' (Arden *et al.* 2019), the contact with frontal and nasal is strongly interdigitated, having an 'M-shape' in dorsal view, unlike the condition of *Irritator*, *Ceratosuchops*, and *Riparovenator*, which have a rough and semicircular surface for nasal contact (Barker *et al.* 2021, Schade *et al.* 2023).

The parietal contact in NHMUK PV R 16423 differs from those other spinosaurids in having a straight transverse posterior margin of the postorbital process, which is posteriorly projected in *Irritator*, *Ceratosuchops*, *Riparovenator*, 'Morph A', and 'Morph B' (Arden *et al.* 2019, Barker *et al.* 2021, Schade *et al.* 2023). However, in the latter 'Morph' the postorbital process is less projected than in other spinosaurids, approaching the condition seen in NHMUK PV R 16423.

Finally, the prefrontal of NHMUK PV R 16423 differs from other spinosaurids in having a 'T-shape' rather than a 'hook-shape', as seen in *Irritator* (Schade *et al.* 2023), *Ceratosuchops*, *Riparovenator* (Barker *et al.* 2021), and *Suchomimus* (Sereno *et al.* 1998). The prefrontal of *Baryonyx* differs from other spinosaurids because it lacks a ventral process (Charig and Milner 1997). The prefrontal cornual process of NHMUK PV R 16423 is also seen in *Ceratosuchops*, *Riparovenator*, and *Suchomimus*, but not in *Irritator* and *Baryonyx* (Charig and Milner 1997, Sereno *et al.* 1998, Barker *et al.* 2021, Schade *et al.* 2023). The angle of the anteroventral process resembles that of *Irritator* (Schade *et al.* 2023), whereas in Baryonychinae the angle of this process is more acute (Charig and Milner 1997, Sereno *et al.* 1998, Barker *et al.* 2021). Based on the aforementioned six synapomorphies shared between NHMUK PV R 16423 and Spinosauridae, we can safely consider this new specimen as belonging to this clade. Furthermore, considering the similarities with *Irritator* and the contemporaneous spinosaurines described by Arden *et al.* (2019), we identify NHMUK PV R 16423 as an indeterminate Spinosaurinae.

Morphological description (axial skeleton)

The dorsal series is represented by a mid-dorsal vertebra that preserves the neural arch and part of the centrum (NHMUK PV R 16430) and a neural dorsal spine lacking its dorsalmost portion (NHMUK PV R 16431). Specimen NHMUK PV R 16430 is interpreted as a middle dorsal vertebra, since the parapophysis is between the neural arch and the centrum, as in the mid-dorsal vertebrae of the spinosaurids *Baryonyx* and *Vallibonavenatrix* (Charig and Milner 1997, Malafaia *et al.* 2020).

The neural spines in both specimens, NHMUK PV R 16430 and NHMUK PV R 16431, are hypertrophied, being large and tall (Figs 7, 8). In lateral view, they are narrower anteroposteriorly expanding dorsally. Dorsal to this expansion, the neural arches become narrower anteroposteriorly and gradually expand dorsally. The neural spines are laterally compressed (Figs 7A–D, 8C–F), projected dorsally or even slightly anteriorly, and their cross-section is quite tabular, being slightly transversely wider anteriorly and at the level of the transverse processes in dorsal view (Fig. 8E, F). Interspinous ligament scars are present and developed similarly on the anterior and posterior surfaces, but the posterior scar extends further dorsally than the anterior (Figs 7A–D, 8C–F). The scars of the interspinous ligament are limited laterally by the spinoprezygapophyseal (e.g. Fig. 8A, B, G, H) and postzygodiapophyseal laminae. The bases of the neural arch in NHMUK PV R 16430 exhibit webs at the level of the spinodiapophyseal fossa (Fig. 7G, H).

The spinoprezygapophyseal laminae extend from the neural spine to the dorsal surface of the bases of the prezygapophyses, delimiting the spinoprezygapophyseal fossa (Figs 7C, D, 8E–H), which is dorsoventrally elongated and deep (e.g. Fig. 8E, F). Spinopostzygapophyseal laminae are also present in both partial vertebrae. These structures are narrower than the spinoprezygapophyseal laminae and extend from the posterior surface of the neural spine to the dorsal margin of the postzygapophyses, reaching the most posterior point of the postzygapophyses (Fig. 7C, D). In both NHMUK PV R 16430 and NHMUK PV R 16431, these laminae delimit the spinopostzygapophyseal fossa, which is similar to the spinoprezygapophyseal fossa but much deeper at the base in NHMUK PV R 16430 (Fig. 7A–D). Only the spinopostzygapophyseal fossa is preserved in NHMUK PV R 16431 (Fig. 8E–H). In NHMUK PV R 16430, the postzygodiapophyseal lamina runs anteriorly from the postzygapophyses to the posterior margin of the transverse processes.

The bases of the transverse processes in NHMUK PV R 16430 are projected laterally and close to the horizontal. These are also dorsoventrally compressed, 'sheet-like' and appear to narrow slightly anteroposteriorly towards the diapophyses (Fig. 7A–F). Under the transverse processes, the neural arch is strongly pneumatized. NHMUK PV R 16430 has both anterior

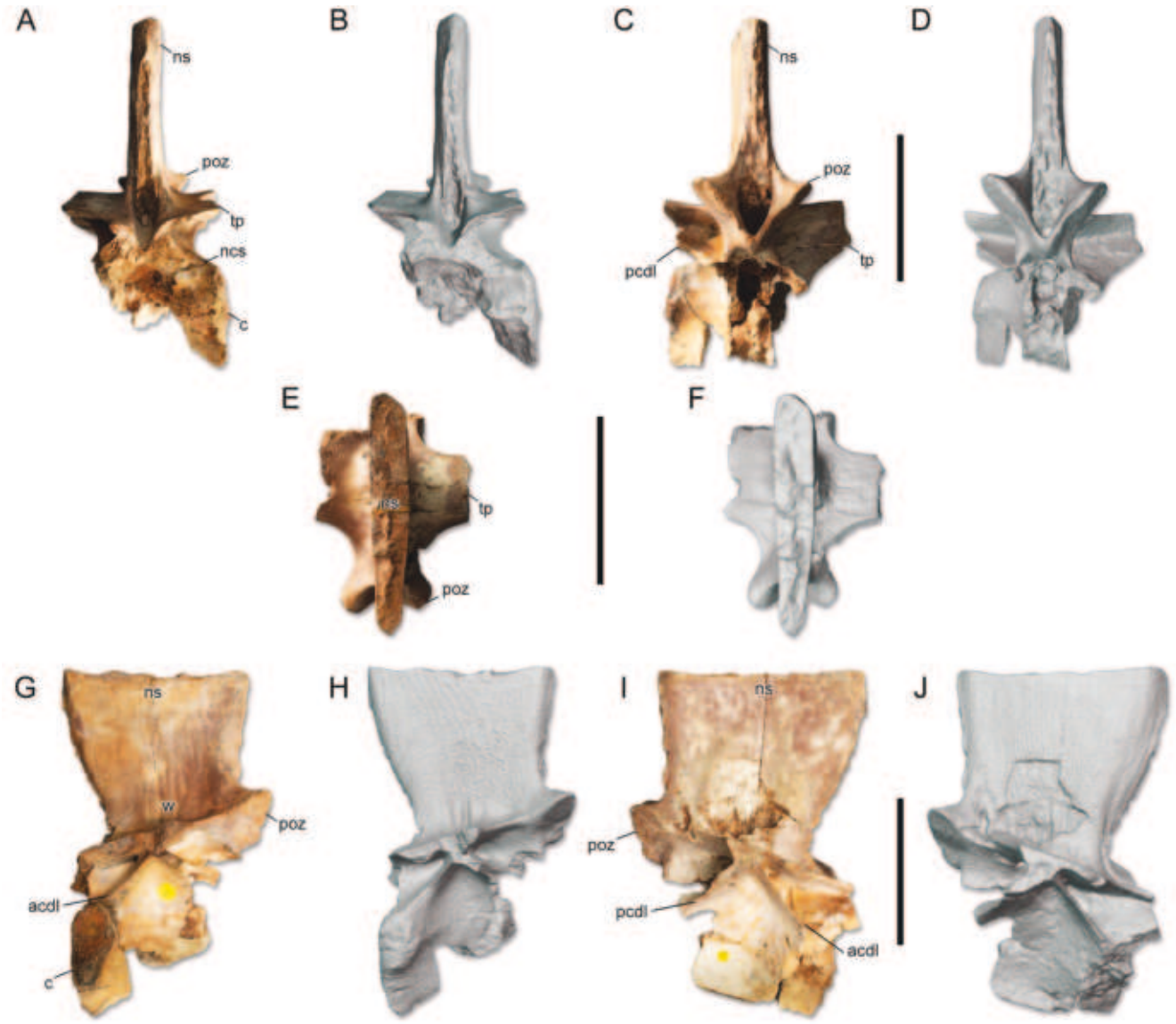

Figure 7. Dorsal vertebra of Spinosaurinae indet. NHMUK PV R 16430. A, B, anterior; C, D, posterior; E, F, dorsal; G, H, right lateral; and I, J, left lateral views. Anatomical abbreviations: acdl, anterior centrodiapophyseal lamina; c, centrum; ncs, neurocentral suture; ns, neural spine; pcdl, posterior centrodiapophyseal lamina; poz, postzygapophyses; tp, transverse process; w, web. Scale bar equals 100 mm.

and posterior centrodiapophyseal laminae (Fig. 7). The anterior centrodiapophyseal lamina extends from the ventral surface of the transverse process and reaches the posterodorsal margin of the parapophysis. The posterior centrodiapophyseal lamina runs from the ventral surface of the transverse process and extends posteroventrally to the centrum (Fig. 7I–J). The anterior centrodiapophyseal lamina is narrower and sharper compared to the more robust and rounded posterior centrodiapophyseal lamina. Adjacent to the transverse processes, three triangular fossae in lateral view are also present. These are the prezygocentrodiapophyseal fossa, the centrodiapophyseal fossa, and the postzygocentrodiapophyseal fossa (Fig. 7G–J). The three fossae are equally deep; however, the centrodiapophyseal fossa is the largest of them. The prezygocentrodiapophyseal fossa is delimited by the prezygodiapophyseal and anterior centrodiapophyseal laminae (Fig. 7G–J). The centrodiapophyseal fossa is delimited by the anterior and posterior centrodiapophyseal laminae, and the postzygocentrodiapophyseal fossa is delimited by the posterior centrodiapophyseal and the postzygodiapophyseal laminae (Fig. 7G–J).

The postzygapophyses project dorsolaterally and their articular surfaces face ventrolaterally. The articular surface of the postzygapophyses is elliptical and flat (Fig. 7C–J). In posterior view, the postzygapophyses are medially fused, but there is no apparent hyposphene.

Morphological comparisons

The base of the NHMUK PV R 16430 vertebra displays the webbing pattern in its spinodiapophyseal fossae, a feature that has been recovered as a synapomorphy of Spinosauridae (Carrano *et al.* 2012, Evers *et al.* 2015, Malafaia *et al.* 2020, Barker *et al.* 2021, Mateus and Estraviz-López 2022, Isasmendi *et al.* 2024). The NHMUK PV R 16430 vertebra does not have the accessory lamina that projects anteroventrally from the posterior

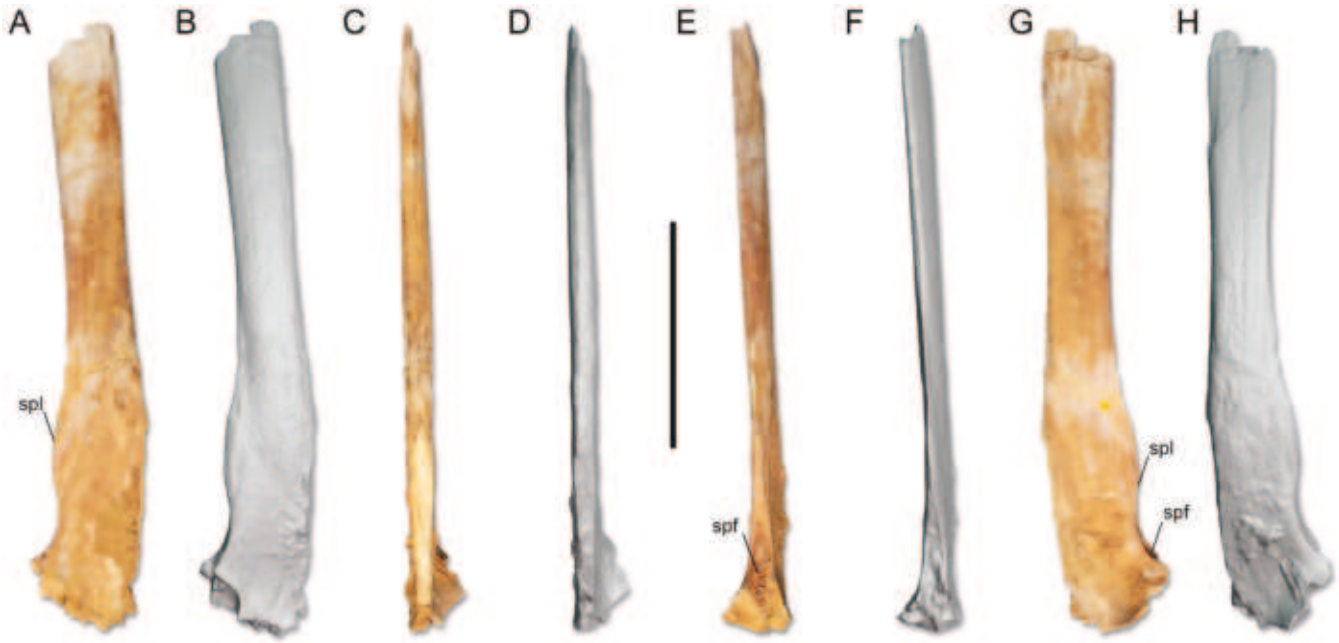

Figure 8. Isolated neural spine of Spinosaurinae indet. NHMUK PV R 16431. A, B, right lateral; C, D, anterior; E, F, posterior; and G, H, left lateral views. Anatomical abbreviations: spf, spinoprezygapophyseal fossa; spl, spinoprezygapophyseal lamina. Scale bar equals 200 mm.

centrodiapophyseal lamina, differing from the middle caudal vertebrae of Baryonychinae species (Sereno *et al.* 1998, 2022, Benson 2010, Allain *et al.* 2012, Carrano *et al.* 2012, Barker *et al.* 2021) or other spinosaurids (e.g. Evers *et al.* 2015, Malafaia *et al.* 2020, Isasmendi *et al.* 2024), and as in *Spinosaurus aegyptiacus*, including the neotype FSAC-KK 11888 (e.g. Carrano *et al.* 2012, Ibrahim *et al.* 2014a, Schade *et al.* 2023).

Furthermore, the hypertrophied dorsal neural spine is much taller than that of non-spinosaurid tetanuran theropods such as *Acrocanthosaurus* (Stovall and Langston 1950), and other spinosaurids such as *Baryonyx*, *Ichthyovenator*, and *Suchomimus* (Charig and Milner 1997, Sereno *et al.* 1998, 2022, Allain *et al.* 2012). Similarly, hypertrophied neural spines occur in the spinosaurines *Spinosaurus aegyptiacus* and FSAC-KK 11888, which are also directed anterodorsally (Stromer 1915, Smith *et al.* 2006, Ibrahim *et al.* 2014a) as the condition noted in NHMUK PV R 16431. The neural spines of the dorsal vertebrae described here further resemble the African spinosaurines, e.g. in NHMUK PV R 16431, the neural spine widens anteroposteriorly near the base of the neural spine, then narrows dorsally, and after this constriction it widens again, but gradually in the same way as occurs in *Spinosaurus aegyptiacus* (Stromer 1915, Smith *et al.* 2006, Ibrahim *et al.* 2014a). Therefore, these specimens closely resemble other contemporary African spinosaurines in morphology [an autapomorphic feature of *Spinosaurus aegyptiacus*; the hypertrophied dorsal neural spine—Stromer (1915), and the webbing (striated) pattern at the base of the neural spine, being a synapomorphic feature of Spinosauridae—Malafaia *et al.* (2020) and Isasmendi *et al.* (2024)]. Thus, both NHMUK PV R 16430 and NHMUK PV R 16431 are referred here as indeterminate Spinosaurinae.

Morphological description (ilia)

The two partial right ilia present different degrees of preservation. The structures that are preserved in both specimens, and therefore overlap, are virtually identical. Specimen NHMUK PV R 16391 preserves the postacetabular blade, the iliac peduncle, the entire brevis fossa, and part of the supra-acetabular crest (Fig. 9); whereas NHMUK PV R 16438 preserves part of the iliac blade, both peduncles, the brevis fossa, and the supra-acetabular crest (Fig. 10).

Specimen NHMUK PV R 16438 has an anteroposterior total length of *c.* 447 mm (Fig. 10). Only the base of the pre-acetabular process is preserved in NHMUK PV R 16438, expanding anteroventrolaterally, providing a smooth 'U-shaped' curvature between the ventral margin of the pre-acetabular blade and the anterior surface of the pubic peduncle (Fig. 10A, B). The portion between the anteroventral process of the ilium and pubic peduncle forms the pre-acetabular notch (or 'cuppedicus' fossa), but does not form a true fossa, as this region is shallow in NHMUK PV R 16438 (Fig. 10A–D). There is no sign of a shelf medial to the pre-acetabular notch. The pubic peduncle of NHMUK PV R 16438 is relatively small and directed ventrally, suggesting a propubic pelvis. Two foramina are on the pubic peduncle. The articulations of the ilium with the pubis and ischium appear to have the same or similar proportions, so both the pubic and ischiatic peduncles are relatively similar in size (Fig. 10A, B). The articular surface of the pubis is triangular in ventral view, being wider in the acetabular region and narrower anteriorly (Fig. 10C, D). Furthermore, the distal outline of the pubic peduncle has its anterior part more ventrally positioned in lateral view, whereas its posterior portion near to the acetabulum is more dorsally positioned, being the anterior limit of the supra-acetabular crest (Fig. 10A, B).

The dorsal surface of the acetabulum is smooth, wide, and slightly straight, presenting a dorsally smooth concave shape in NHMUK PV R 16438. In ventral view, its supra-acetabular crest is completely preserved, projecting from the posterolateromedial portion of the ischiatic peduncle to form the posterolateral

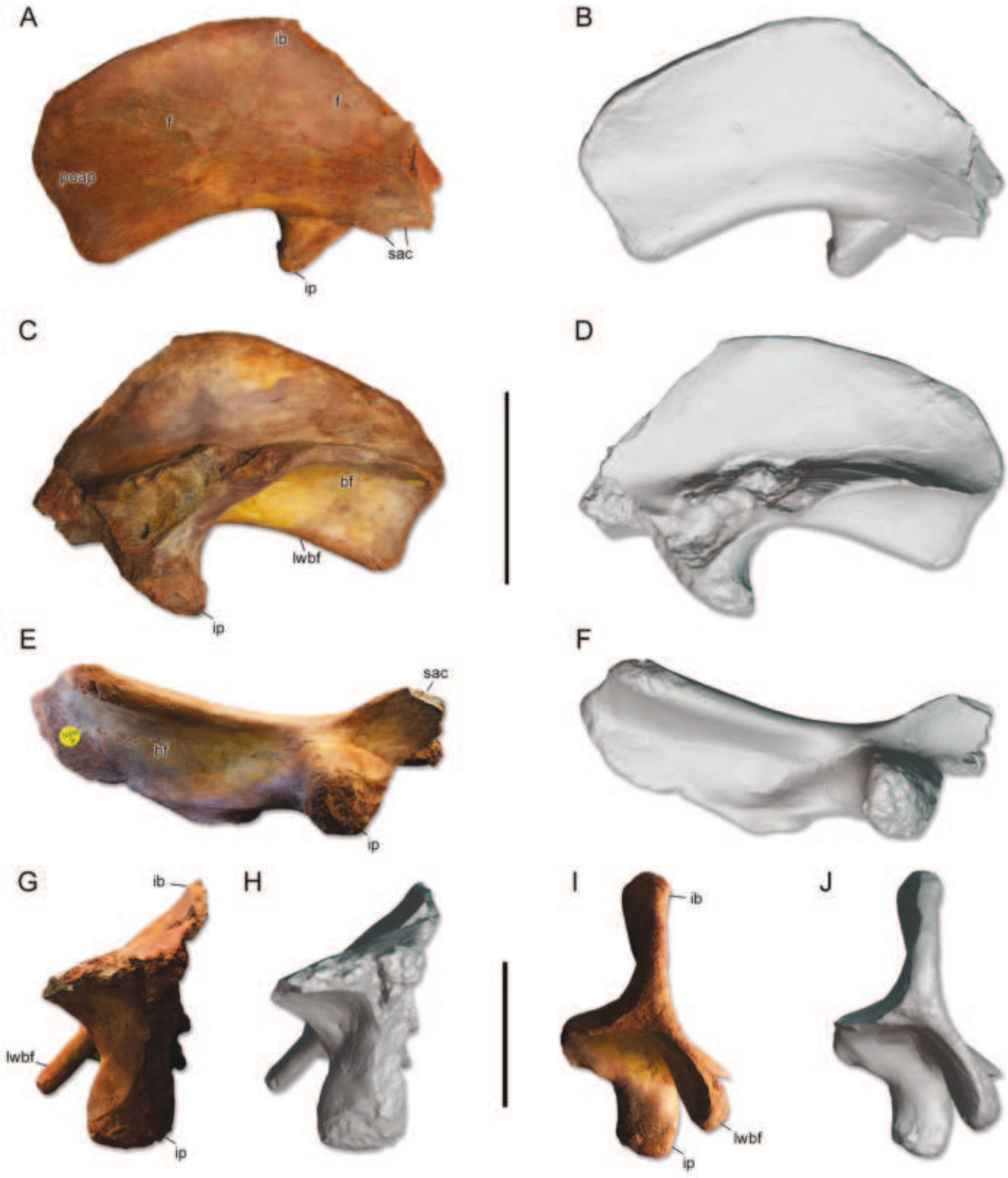

Figure 9. Ilium of Spinosaurinae indet. NHMUK PV R 16391. A, B, right lateral; C, D, medial; E, F, ventral; G, H, anterior; and I, J, posterior views. Anatomical abbreviations: bf, brevis fossa; f, foramen; ib, iliac blade; ip, ischiadic peduncle; lwbf, lateral wall of the brevis fossa; poap, postacetabular process; sac, supra-acetabular crest. Scale bar equals 200 mm (A–F) and 100 mm (G–H).

acetabular edge of the pubic peduncle (Fig. 10A–D). The supra-acetabular crest is directed ventrolaterally, being well developed but not a large/pendant 'hood' (*sensu* Carrano *et al.* 2012), with an ovoid outline, and occluding the anteroventral region of the acetabulum in lateral view (Fig. 10C, D). In the specimen NHMUK PV R 16391 (total length of *c.* 430 mm), the supra-acetabular crest projects from the posterolateral portion of the ischiatic peduncle (slightly more posterior than in NHMUK PV

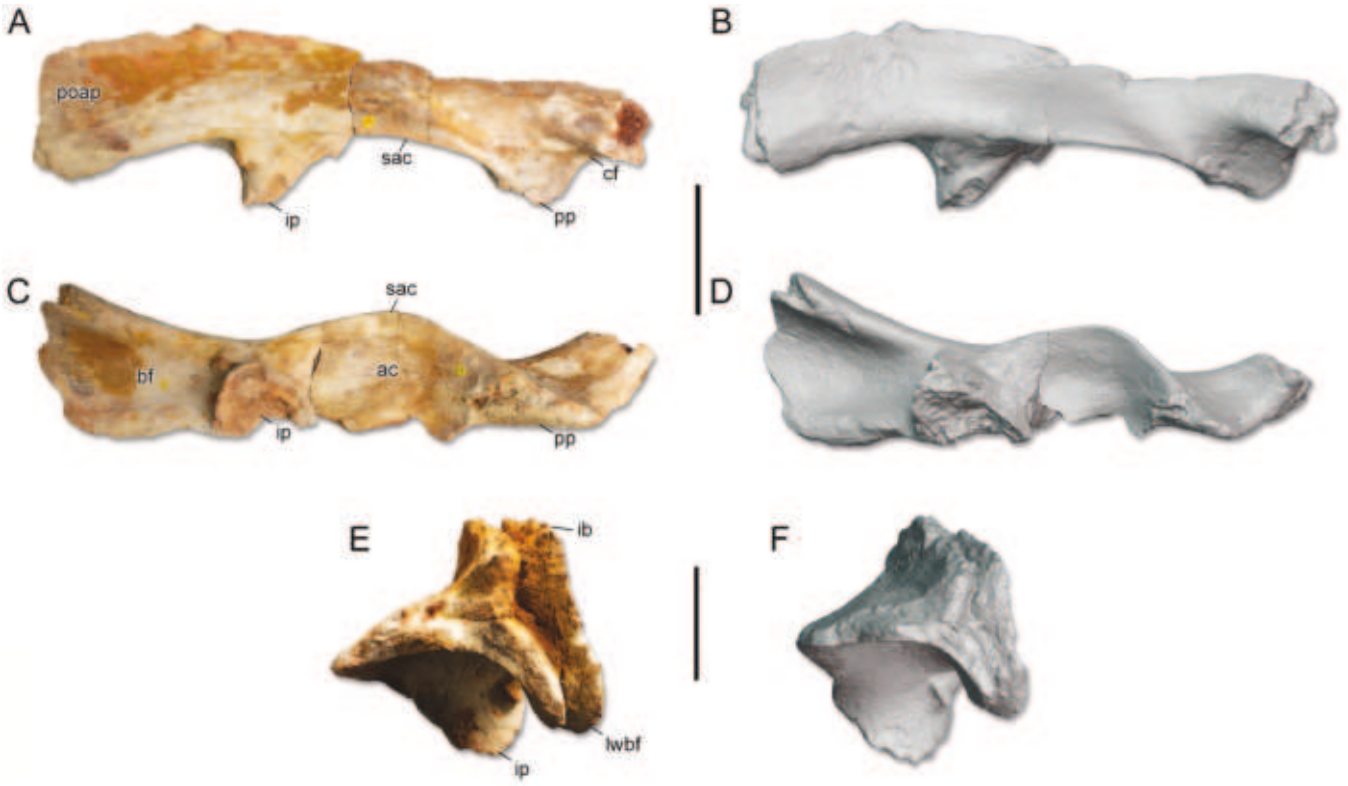

Figure 10. Ilium of Spinosaurinae indet. NHMUK PV R 16438. A, B, right lateral; C, D, ventral; and E, F, posterior views. Anatomical abbreviations: ac, acetabulum; bf, brevis fossa; cf, 'cuppedicus fossa'; ib, iliac blade; ip, ischiadic peduncle; lwbf, lateral wall of the brevis fossa; pp, pubic peduncle; poap, postacetabular process; sac, supra-acetabular crest. Scale bar equals 100 mm.

R 16438), also being a well-developed and short crest directed anterolaterally, but only the posterior part is preserved (Fig. 9A–F).

On the posterolateral surface of both ilia, there is a gap that separates the supra-acetabular crest and the most anteroventral part of the brevis shelf in the postacetabular blade, posterior to the ischiatic peduncle (Figs 9E, F, 10C, D). The brevis shelf is a cylinder-like bony bar; more pronounced posteriorly; giving it a 'lobular' appearance in posterior view (Fig. 9I, J). The ischiatic peduncle is directed anteroposteriorly; its anterior acetabular surface is flat (particularly in the better-preserved specimen NHMUK PV R 16391), while the posterior surface is concave with the distal end tapering posteroventrally (Figs 9A, B, 10A, B). Thus, the outline of the ventral border of the brevis shelf and the posterior edge of the ischiatic peduncle is 'hook-shaped' (Fig. 9A–D). The distal facet of the ischiatic peduncle in NHMUK PV R 16391 is rounded and NHMUK PV R 16438 has its distal ischiatic peduncle eroded medially; however, it still seems to have a rounded morphology.

The postacetabular length in relation to the length of the ischiatic peduncle is greater than 1 in both specimens, being a deep process projected posteroventrolaterally with a straight outline (Figs 9A–D, 10A, B). In the most ventral postacetabular blade, the lateral wall of the brevis fossa is high throughout its entire length, thus, the medial wall of the fossa is concealed in lateral view (Figs 9A–D, 10A, B). The brevis fossa is located ventrally in the postacetabular blade, posterior to the ischiatic peduncle and restricted to the lateral and medial wall of the brevis fossa. This is relatively deep and wide, becoming posteriorly wider. The lateral wall of the fossa is expanded laterally in anterior view, contributing to the posterior widening of the brevis fossa (Figs 9, 10C, D). In posterior view, the lateral wall of the brevis fossa is oblique relative to the main axis of the ischiatic peduncle, while the medial wall is almost horizontal and directed ventromedially (Figs 9I, J, 10E, F).

At least two foramina can be seen on the lateral surface of the iliac blade of NHMUK PV R 16391, one positioned anteriorly at the same level as the anterior surface of the ischiatic peduncle and the other positioned posteriorly at the medial level of the postacetabular process (Fig. 9A, B).

Dorsal to the supra-acetabular crest, some radial scars are present on the iliac blade, reminiscent of muscular origins. The preserved part of the iliac blade is flat and smooth in NHMUK PV R 16391 (Fig. 9A, B) and NHMUK PV R 16438; thus, there is no sign of a vertical ridge on the ilium. In lateral view, the shape of the dorsal margin of the ilium is convex. In dorsal view, the outline of the dorsal edge of the ilium has a sigmoid shape; more laterally expanded posteriorly, and directed medially becoming anteriorly projected (or straight) in the most anterior region of the dorsal border. This straighter dorsal part can also be seen in lateral view, where the anterior portion is flatter dorsoventrally, softening the curve of the dorsal outline of the ilium anteriorly (Fig. 9A, B). In this way, the dorsal edge of the postacetabular process and its ventral edge become parallel (Fig. 9A, B).

In the dorsoposterior border of the postacetabular process, NHMUK PV R 16391 presents the *crista dorsolateralis ilii* (*sensu*

Baumel and Witmer 1993) of the ilium well preserved, in addition to the muscle–bone contact area, which is rough, presenting some undulations of the bone surface (Fig. 11). Such characteristics are the osteological correlates of the most superficial and posterior muscles of the thigh *M. iliotibialis 3* (IT3; level I inference of Witmer 1995).

The shape of the posterior surface of the postacetabular process in NHMUK PV R 16391 is convex; however, its posterior border is asymmetrical, with its posterodorsal margin flattening posteriorly ventrally and projecting posteriorly (but not as much as in *Megalosaurus*; Benson 2010, Lacerda *et al.* 2023). This posterior projection occurs at the level of contact with the medial wall of the brevis fossa. The morphology of the posteroventral edge of the postacetabular process is straight (Fig. 9A–D). Although specimen NHMUK PV R 16438 has its postacetabular process more eroded, its posteroventral edge is also straight (Fig. 10A, B).

The medial surface of NHMUK PV R 16391 is well preserved. The medial wall of the brevis shelf, as previously noted, is quite horizontal, being an arched structure; its posterior limit is in the region of greatest posterior expansion of the ilium, becoming more dorsal anteriorly, and thus participating in the deepening of the brevis fossa (Fig. 9C, D). The medial wall occludes the brevis fossa anteriorly, as this structure becomes more ventrally projected, mainly in the probable contact with the sacral vertebra 1 (in an irregular and striated region), and anteriorly in the contact with the sacral vertebra 2, located adjacent to the ischiatic peduncle (Fig. 9C, D).

Morphological comparisons

In a number of features, both NHMUK PV R 16391 and NHMUK PV R 16438 resemble Tetanurae in: (i) the presence of a reduced ventrolateral supra-acetabular crest, occluding the anterodorsal portion of the acetabulum; (ii) ventrally oriented pubic peduncle (also seen in ceratosaurs); (iii) convex shape of the dorsal margin of the ilium; and (iv) the morphology between the supra-acetabular crest and the brevis shelf, on the lateral surface, as a gap (differing from the continuous ridge of ceratosaurs) (Hutchinson 2001b, Benson 2010, Carrano *et al.* 2012, Cuesta *et al.* 2018, Malafaia *et al.* 2020, Lacerda *et al.* 2023). Moreover, the presence of a shallow pre-acetabular notch, not forming a true fossa, as well as the lack of a ridge on the ilium, just medial to the pre-acetabular notch, which can be considered based on the NHMUK PV R 16438 specimen, indicates differences between this individual and taxa of Avetheropoda (*sensu* Hutchinson 2001b, Benson 2010, Carrano *et al.* 2012, Malafaia *et al.* 2020). The presence of a brevis fossa that widens posteriorly differentiates both ilia described here from metriacanthosaurid avetheropods (Carrano *et al.* 2012, Lacerda *et al.* 2023).

Based on their combination of morphological features, both ilia described here more closely resemble the general morphology of spinosaurids than other theropods. Similar to the spinosaurid *Ichthyovenator* (Allain *et al.* 2012), both ilia related to North African spinosaurines (FSAC-KK 11888 and MSNM V6900; Ibrahim *et al.* 2014a), as well as the indeterminate specimen MN 4819-V (Machado 2010), both NHMUK PV R 16391 and NHMUK PV R 16438 do not present any sign of a vertical ridge on the lateral surface of the ilium. This differs from the spinosaurids *Vallibonavenatrix* (Malafaia *et al.* 2020) and *Suchomimus*, which present a low ridge, and later-diverging metriacanthosaurids, which have a double ridge (Carrano *et al.* 2012, Lacerda *et al.* 2023).

The moderately ventromedial extension of the supra-acetabular crest and its outline morphology in ventral view in NHMUK PV R 16438 resemble spinosaurids such as *Vallibonavenatrix* and the lateral morphology of this crest is also similar to, for instance, *Vallibonavenatrix*, *Ichthyovenator*, and *Suchomimus* (Allain *et al.* 2012, Malafaia *et al.* 2020, Lacerda *et al.* 2023).

The brevis shelf as a cylinder-like bony bar ventrally is also seen in *Ichthyovenator* (Allain *et al.* 2012), *Vallibonavenatrix* (less robust) (Malafaia *et al.* 2020), MSNM V6900, and probably *Suchomimus*; besides this, the shape of the brevis fossa—widening posteriorly—is also shared among spinosaurids (except *Ichthyovenator*) and both NHMUK PV R 16391 and NHMUK PV R 16438. However, the widening of the brevis fossa is homoplastic in theropods (Lacerda *et al.* 2023). Several theropods have the lateral wall of the brevis fossa shorter than the

Figure 11. *Crista dorsolateralis ilii* (osteological correlate of *M. iliotibialis 3*) on the ilium of Spinosaurinae indet. NHMUK PV R 16391. Scale bar equals 20 mm.

medial wall anteriorly, exposing the medial wall in lateral view. In both ilia, the lateral wall is taller along its entire length, hiding the brevis fossa in lateral view, as occurs in the spinosaurids *Suchomimus*, FSAC-KK 11888 and MSNM V6900 (Ibrahim *et al.* 2014a). The shape of the brevis fossa in posterior view and its medial and lateral walls in NHMUK PV R 16391 is identical to the morphology of the FSAC-KK 11888 specimen by having a horizontal medial wall, and the posterolateroventrally directed distal portion forming the 'lobular-like' lateral wall of the brevis fossa.

NHMUK PV R 16391 also shares with *Suchomimus*, FSAC-KK 11888, and probably also MSNM V6900 a flat and dorsally convex shape of the dorsal rim of the postacetabular process of the ilium. Although the posterior outline of the postacetabular is convex in NHMUK PV R 16391 and other spinosaurids (but also avetheropods). The shape of the ilia described here resembles more the morphology of FSAC-KK 11888 and MSNM V6900 than other specimens, by having an asymmetrical posterior surface of the postacetabular process, with its posterodorsal margin flattening ventroposteriorly and projecting posteriorly (but not as much as in *Megalosaurus*; Benson 2010, Lacerda *et al.* 2023) and the straight posteroventral edge of the postacetabular process. Nevertheless, the shape of the posterior facet of the ischiatic peduncle, as well as the posteroventrolaterally directed lateral wall of the brevis fossa, giving it a 'hook-shaped' posteroventral outline. This shape is similar among NHMUK PV R 16391, NHMUK PV R 16438, and the spinosaurines FSAC-KK 11888 and MSNM V6900. In lateral view, the ventral margin of the postacetabular process is straight in spinosaurids, such as *Ichthyovenator*, *Suchomimus*, and FSAC-KK 11888. Moreover, this margin is ventrally directed posteriorly; the same morphology noted in NHMUK PV R 16391 and NHMUK PV R 16438.

Interestingly, among tetanurans a feature noted only in NHMUK PV R 16438 and spinosaurines, such as FSAC-KK 11888, MSNM V6900, and the Brazilian specimen MN 4819-V (Machado 2010), is the morphology of the pubic peduncle and its relative size with the ischiatic peduncle. Generally, tetanurans have the pubic peduncle larger than the ischiatic peduncle. This can be 130% larger or more, and most of these theropods have a distal pubic expansion (Hutchinson 2001b, Benson 2010, Allain *et al.* 2012, Carrano *et al.* 2012, Malafaia *et al.* 2020, Lacerda *et al.* 2023, 2024). As previously mentioned, the exceptions noted by Malafaia *et al.* (2020) are the spinosaurines, which have both iliac peduncles similar in proportion. Concerning the ilium FSAC-KK 11888, Lacerda *et al.* (2023) considered the pubic peduncle slightly larger than the ischiatic, whereas Malafaia *et al.* (2020) considered both at the same proportions. In spite of that, a small pubic peduncle is only found in the Spinosaurinae clade among Tetanurae, this being the same feature noted in NHMUK PV R 16438.

Finally, the (*M. iliotibialis 3*) muscle scar on the dorsal rim of the postacetabular blade, noted in NHMUK PV R 16391, is similar in topology with other theropods (e.g. Carrano and Hutchinson 2002), and the rough pattern is similar to other megalosauroids (Lacerda *et al.* 2024).

Thus, based on the several features described and the similarities with spinosaurine theropods, we refer both NHMUK PV R 16391 and NHMUK PV R 16438 as indeterminate Spinosaurinae individuals.

Morphological description (femur)

Specimen NHMUK PV R 16433 is a well-preserved left femur, missing only the distal end (Fig. 12). The femur is *c.* 371 mm in length. The femoral shaft, in anterior and posterior views, has a straight shape (Fig. 12A–C); in medial and lateral views, it curves markedly posteriorly (Fig. 12E–H), being especially arched in the most distal portion of the diaphysis. Thus it is sigmoid in medial and lateral views (Fig. 12E–H). The transverse section of the diaphysis (based on a distal break) is elliptical in shape.

The femoral head is positioned *c.* 15° anteromedially (in dorsal view; Fig. 12I, J) relative to the posterior edge of the proximal portion of the distal condyles (not shown in Fig. 12I, J), and oriented medially (based on the main axis of the diaphysis), with the dorsal surface positioned horizontally in anterior view (Fig. 12A, B). The femoral neck is well developed. The medial articular surface of the femoral head is straight, tapering distally, having an irregular and almost oval shape (Fig. 12G, H). On the posterior surface of the caput there is a longitudinal groove that slopes laterally in the distal portion. The distolateral delimitation of this groove appears to be the base of the flange of the caput; however, this region may have suffered abrasion (Fig. 12C, D). There is a shallow portion on the posterior surface of the femoral head in NHMUK PV R 16433, which seems to be homologous with the oblique ligament groove in theropods (e.g. Carrano *et al.* 2012, Malafaia *et al.* 2018). In dorsal view, the head has a straight posterior surface and an arched anterior surface, becoming mediolaterally narrow towards the greater trochanter (Fig. 12I, J).

The greater trochanter is continuous with the femoral head. It is wide and posterolaterally expanded in its distal portion, forming a smooth and rounded junction with the posteroproximal femoral shaft (Fig. 12C, D). The junction of the greater trochanter in the anteroproximal region of the diaphysis becomes even smoother with the distal narrowing of the greater trochanter (Fig. 12E, F).

The lesser trochanter is robust and relatively thick, especially in the distal region at its junction with the femoral shaft, being more tapered posteroproximally near the cleft that separates this structure from the greater trochanter (Fig. 12A, B I, J). The proximal contact of the lesser trochanter with the greater trochanter is smooth, and the cleft that divides these structures is shallow. The lesser trochanter forms a wide semi-oval flange. Its dorsal edge is 'U-shaped' and its proximal end slightly exceeds the ventral margin of the femoral head (Fig. 12A, B). The anterolateral surface of the lesser trochanter is flat, while its anteromedial surface is irregular. The accessory trochanter projects slightly anterodistally from the lesser trochanter, but this is a poorly developed structure represented by a thickening of the distal margin, giving an irregularly arched shape to the anterior edge of the lesser trochanter (Fig. 12A, B E, F). At the laterodistal base of the lesser trochanter, a distinct trochanteric shelf is present, formed by a smooth protuberance, located on the lateral surface of the diaphysis, proximal to the fourth trochanter (Fig. 12C–F). These structures border a shallow concavity between the distolateral greater trochanter, the posterior surface of the lesser trochanter, and the proximal edge of the trochanteric shelf (Fig. 12E, F).

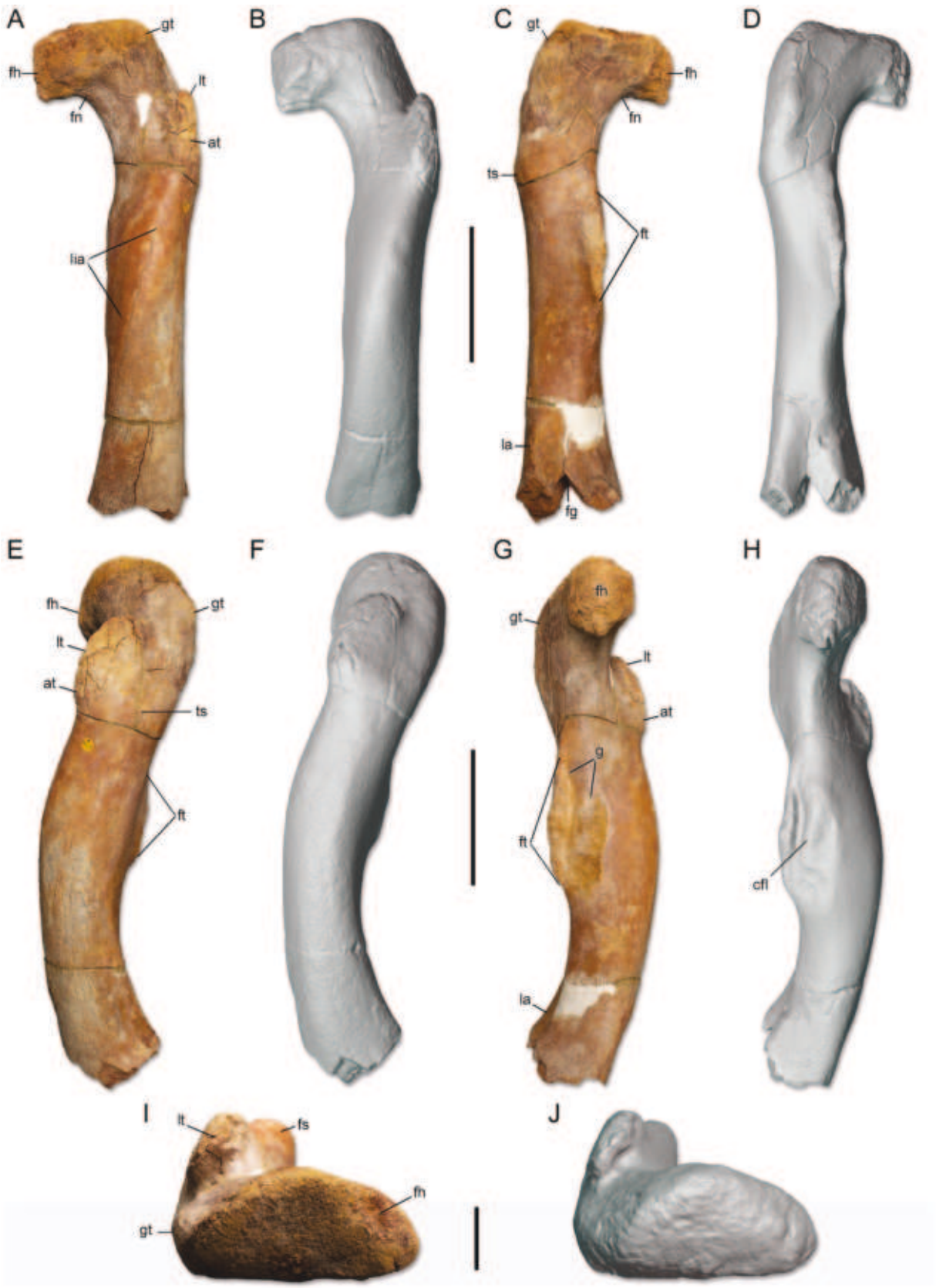

Figure 12. Femur of Spinosaurinae indet. NHMUK PV R 16433. A, B, anterior; C, D, posterior; E, F, lateral; G, H, medial; and I, J, dorsal views. Anatomical abbreviations: at, accessory trochanter; cfl, *M. caudofemoralis longus* insertion scar; fh, femoral head; fg, flexor groove; fn, femoral neck; ft, fourth trochanter; g, groove; gt, greater trochanter; la, *linea aspera*; lia, *linea intermuscularis cranialis*; lt, lesser trochanter; ts, trochanteric shelf. Scale bar equals 100 mm (A–H) and 30 mm (I–J).

The fourth trochanter is hypertrophied and appears as a prominent elliptical-shaped flange, being longer proximodistally than anteroposteriorly and occupying one-third of the femur (Fig. 12G, H). Proximally, the fourth trochanter originates smoothly near the level of the distal base of the lesser trochanter and expands proximodistally to the medial region of the femoral shaft, ending in a gentle curve (Fig. 12G, H). In lateral view, the fourth trochanter protrudes slightly, having a straight outline (Fig. 12E, F). A protrusion is present on the most posterior rim of the fourth trochanter, being slightly asymmetrical and positioned distally (Fig. 12G, H).

The posterolateral surface of the fourth trochanter is smooth, while the posteromedial surface is irregular with a well-marked keel separating two depressions: (i) a deeper and narrower sulcus that extends longitudinally and parallel to the fourth trochanter at its base, originating in the proximal portion and occupying at least two-thirds of the fourth trochanter; and (ii) a shallower and wider depression, located medial to the fourth trochanter and the sulcus previously mentioned. It originates approximately at the medial height of the proximal fourth trochanter (more distal than the longitudinal sulcus), widening distally and becoming shallower at the distal base of the fourth trochanter (Fig. 12G, H). Both depressions represent osteological correlates related to the attachment of strong hip extensor muscles (e.g. Gatesy 1990, Hutchinson 2001a, Carrano and Hutchinson 2002). Based on the femur NHMUK PV R 16433, we infer that the entire lateral surface of the fourth trochanter was the region of insertion of the *caudofemoralis brevis* muscle (CFB); whereas the medial surface of the fourth trochanter, the medial sulcus, and the large elliptical groove on the medial side was a broad insertion for a large *caudofemoralis longus* muscle (Fig. 12G, H). Both *Mm. caudofemorales* are a level II inference by Witmer's (1995) systematization, being in positions topologically similar to other theropods (e.g. ceratosaurs—Cerroni *et al.* 2024, early tetanurans—Lacerda *et al.* 2024, and late-diverging coelurosaurs—Carrano and Hutchinson 2002).

Distally, the posterior region of the femoral shaft is straight and expands slightly mediolaterally at the distal end, proximally to where the condyles would be (Fig. 12A–D). On the medial and distal surfaces of the femur, the anteromedial (or 'craniomedial distal') crest is rounded and poorly developed. NHMUK PV R 16433 also has a poorly developed, rounded medial epicondyle (or medial distal crest) (Fig. 12C, D). Although the distal condyles are not preserved, distally the femoral shaft, in posterior view, forms a gap that separates two posterior elevations, which probably represent the proximal border of the linea aspera (which is visible in anterior view; Fig. 12A, B) on the medial side of the tibiofibular crest; therefore, being homologous to the flexor groove of other theropods (e.g. Hutchinson 2001a, Benson 2010).

Morphological comparisons

Specimen NHMUK PV R 16433 shares several features with tetanuran theropods, such as: (i) the femoral head positioned anteromedially and oriented medially; (ii) the dorsal edge of the lesser trochanter slightly surpassing the ventral margin of the femoral head; (iii) the reduced trochanteric shelf; and (iv) the lesser trochanter resembling a wide flange (Gauthier 1986, Hutchinson 2001a, Benson 2010, Carrano *et al.* 2012, Cuesta *et al.* 2018, Lacerda *et al.* 2023).

In the specimen studied here, the position and orientation of the femoral head differs from most allosauroids, such as the metriacanthosaurid *Neovenator* and the carcharodontosaurids *Acrocanthosaurus* and *Carcharodontosaurus*, and *Giganotosaurus*, being oriented medially and at a dorsomedial angle in the latter (Stromer 1931, Carrano *et al.* 2012, Cuesta *et al.* 2018, Lacerda *et al.* 2023). A femoral head positioned anteromedially and oriented medially is shared between NHMUK PV R 16433 and both megalosauroid and metriacanthosaurid tetanurans (Charig and Milner 1997, Benson 2010, Machado 2010, Carrano *et al.* 2012, Malafaia *et al.* 2018, Lacerda *et al.* 2023).

Interestingly, there is only a very shallow portion on the posterior surface of the femoral head in NHMUK PV R 16433, which may be homologous with the groove of the oblique ligament. In theropods, it is generally represented by a deep and bounded structure, except in the megalosauroids *Afrovenator*, *Megalosaurus*, *Torvosaurus*, and FSAC-KK 11888, which only have a shallow groove (Benson 2010, Carrano *et al.* 2012, Lacerda *et al.* 2023).

In non-Avetheropoda theropods, including African spinosaurine FSAC-KK 11888 (Lacerda *et al.* 2023) and NHMUK PV R 16433, the accessory trochanter (which derives from the lesser trochanter), is represented by a weak structure that forms the slightly thickened margin of the lesser trochanter. This is the condition observed in NHMUK PV R 16433, which differs from the spinosaurid *Suchomimus* and also Avetheropoda taxa in general, which have the accessory trochanter as a triangular flange (Benson 2010, Carrano *et al.* 2012, Sereno *et al.* 2022, Lacerda *et al.* 2023).

NHMUK PV R 16433 also shares with spinosaurids (and other megalosauroids) the rounded and poorly developed morphology of the medial epicondyle, which differs from the ridge-shaped structure present in ceratosaurs and allosauroids (Allain *et al.* 2007, Benson 2010, Carrano *et al.* 2012, Evans *et al.* 2015, Malafaia *et al.* 2018, Sereno *et al.* 2022, Lacerda *et al.* 2023, 2024, Cerroni *et al.* 2024, Isasmendi *et al.* 2024).

Based on the four main characteristics of the proximal femur described previously, along with the presence of a low and rounded medial epicondyle and the probably shallow groove of the oblique ligament, it is possible to assign the NHMUK PV R 16433 femur to the Megalosauroidea clade. Within this clade, NHMUK PV R 16433 more closely resembles the morphology of spinosaurids than that of other megalosauroids.

The overall shape of the femoral head in NHMUK PV R 16433 resembles the spinosaurids *Baryonyx*, FSAC-KK 11888, *Suchomimus* (Ibrahim *et al.* 2014a, Sereno *et al.* 2022, Lacerda *et al.* 2023), and specimens MN 4819-V (Machado 2010) and CMP-MS-0/22 (Malafaia *et al.* 2018). The medial surface of the femoral head in NHMUK PV R 16433 resembles the shape of *Suchomimus* more than in FSAC-KK 11888, as it has a horizontal and continuous dorsal surface of the femoral head, which is less arched on its anterior edge, as seen in dorsal view. Nevertheless, the remainder of the proximal femoral morphology described here is similar to that observed in FSAC-KK 11888. Similarities between FSAC-KK 11888 and NHMUK PV R 16433 include: (i) greater trochanter morphology; (ii) position and

morphology of the lesser trochanter, which has a weak accessory trochanter forming only a thick distal margin (differing from MN 4819-V—Machado 2010 and *Suchomimus*—Lacerda *et al.* 2023); (iii) position and shape of the trochanteric shelf; (iv) the overall shape and position of the fourth trochanter; and (v) degree of anteroposterior curvature of the femoral shaft, which is markedly curved in FSAC-KK 11888, NHMUK PV R 16433, and probably *Riojavenatrix*, than in *Suchomimus* and CMP-MS-0/22 (Ibrahim *et al.* 2014a, Malafaia *et al.* 2018, Sereno *et al.* 2022, Isasmendi *et al.* 2024). Furthermore, based on the muscles that were inserted on to the fourth trochanter of NHMUK PV R 16433, it is possible to infer that the Mm. caudofemorales represented relatively robust muscles (or the tendons thereof) in this specimen. The osteological correlates are much more evident than in other megalosauroids (e.g. piatnitzkysaurids—Lacerda *et al.* 2024), which potentially is consistent with the proposal of a robust and strong tail in the African spinosaurine described by Ibrahim *et al.* (2020a), and topologically similar to the femur FSAC-KK 11888. Thus, the morphology of the specimen studied here is more similar to that of FSAC-KK 11888 and other spinosaurids than that of other theropods; on this basis, NHMUK PV R 16433 is interpreted as representing an indeterminate Spinosaurinae.

Sigilmassasaurus Russell, 1996

Type-species: *Sigilmassasaurus brevicollis*

Sigilmassasaurus brevicollis

(Fig. 13)

Referred specimen

A completely preserved posterior cervical vertebra (NHMUK PV R 38358).

Morphological description

NHMUK PV R 38358 is an almost complete cervical vertebra, with only part of the neural spine missing. Based on the axial sequence proposed by Evers *et al.* (2015), NHMUK PV R 38358 can be identified as a C9 (Fig. 13).

The vertebral centrum is *c.* 125 mm long anteroposteriorly, *c.* 140 mm wide, and *c.* 95 mm high. It is strongly opisthocoelous and the anterior articular surface is surrounded by a rim (Fig. 13A, B). NHMUK PV R 38358 has a vertebral centrum that is shorter than it is wide, being 12% wider than it is long, and its dorsal surface is slightly anteroposteriorly shorter than ventral surface. The articular facets are wide, with the anterior and the posterior articular surfaces being 1.4 and 1.6 times wider than they are tall, respectively (Fig. 13). The anterior articular surface is strongly convex and the posterior one is strongly concave. In anterior view, the anterior articular surface is pronouncedly elliptical (Fig. 13A, B) and, in posterior view, the posterior one has a reniform outline (Fig. 13C, D). The ventral surface exhibits a well-developed ventral keel that extends to the anterior and posterior margins of the vertebral centrum, widening slightly transversely towards these edges (Fig. 13G, H). In lateral view, the anterior and posterior parts of the keel project further ventrally, so that it is concave at midlength of the centrum (Fig. 13I–L). Anteriorly, the ventral keel gradually becomes lower and merges into a small, rough, triangular area located immediately anterior to the parapophyses (Fig. 13G, H). Lateral to the ventral keel, a fossa is present on each side of the centrum. These fossae are delimited anterolaterally by the parapophyses and the lamina that connects the parapophyses to a small anterior triangular area, and posterolaterally by a lamina that extends from the parapophyses posteriorly to the posterior articular facet (Fig. 13G–L). No hypapophysis seems to be present in NHMUK PV R 38358.

The parapophyses are robust, 'button-shaped' structures that are long and project ventrolaterally; located anteroventrally on the lateral surfaces of the centrum (Fig. 13A–D, G–L). The articular surfaces of the parapophyses are concave and oval in outline. From the posterior margin of each of the parapophyses, a rounded ridge extends posteriorly; these are the ridges that laterally delimit the ventral fossae (Fig. 13G, H). Above the parapophyses, a single and large central pneumatic foramen is present on each side of the NHMUK PV R 38358 vertebral centrum and it penetrates the bone anteroventrally (Fig. 13I–L). Each foramen has a different shape: the right one is triangular and anteroposteriorly larger than tall (Fig. 13), whereas the left is oval and taller than its length anteroposteriorly (Fig. 13K, L).

The neurocentral suture in NHMUK PV R 38358 is still visible. The neural canal is large, subrectangular to oval in shape, and transversely wider than tall (Fig. 13A–D). The pleurocentral depressions are located ventral to this suture, anterodorsally located on the centrum.

The transverse processes are very large and project ventrolaterally at an angle of *c.* 40° to the lateral surface (Fig. 13A–D). In anterior view, the transverse processes are quite straight dorsoventrally (their dorsal surfaces are distinctly flat), but towards the diapophyses they curve slightly more ventrally. In dorsal view, the posterior surfaces of the transverse processes are straight and laterally directed (Fig. 13E, F). The anterior margin is gently concave in dorsal view and expands anteriorly near the diapophyses. The diapophyses face ventrolaterally and are convex and triangular in outline. Both prezygodiapophyseal and postzygodiapophyseal laminae are present. These laminae are robust, rounded, developed in a similar way, and are less marked near the diapophysis. The prezygodiapophyseal lamina extends laterally from the anterolateral margin of the prezygapophyses along the anterodorsal margin of the transverse process, reaching the anterodorsal margin of the diapophyses. The postzygodiapophyseal lamina runs from the anterolateral margin of the postzygapophyses toward the diapophyses, forming the posterodorsal edge of the transverse process. The centroprezygapophyseal lamina is directed anterolaterally and merges with the prezygodiapophyseal lamina on the anterior surface of the base of the prezygapophyses, with the lamina being less marked, but more robust and rounded than the prezygodiapophyseal lamina.

The centrodiapophyseal lamina is present on the ventral surface of the transverse process. This is very prominent and it seems not to be bifurcated into the anterior centrodiapophyseal and posterior centrodiapophyseal laminae. However, there is another lamina that runs from the ventral surface of the transverse process toward the posterodorsal margin of the centrum [probably the posterior centrodiapophyseal lamina according to

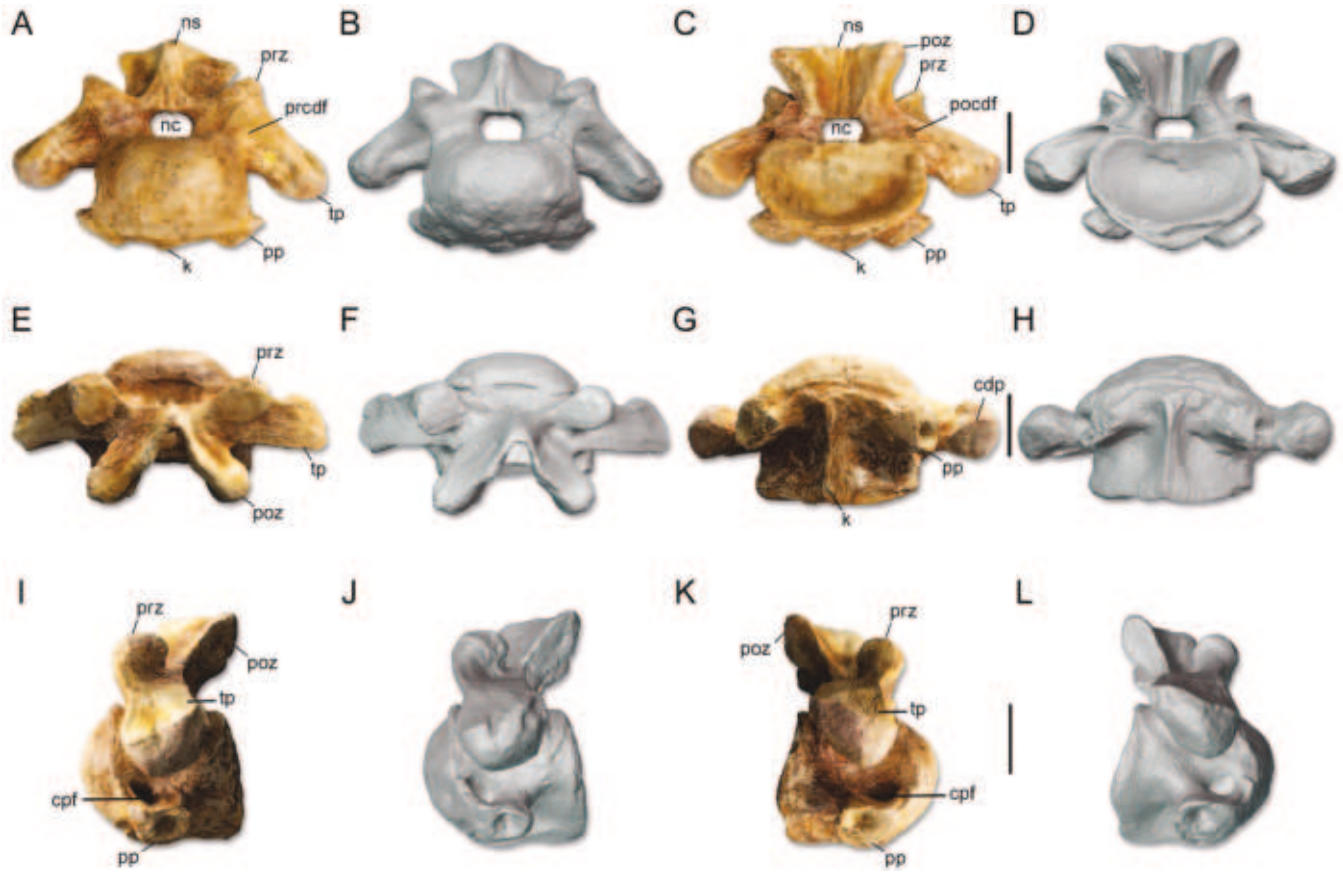

Figure 13. Cervical vertebra (C9) of *Sigilmassasaurus brevicollis* NHMUK PV R 38358. A, B, anterior; C, D, posterior; E, F, dorsal; G, H, ventral; I, J, left lateral; and K, L, right lateral views. Anatomical abbreviations: cpf, central pneumatic foramen; cdp, centrodiapophyseal lamina; k, keel; nc, neural canal; ns, neural spine; pp, parapophyses; pocdf, postzygocentrodiapophyseal fossa; poz, postzygapophyses; prcdf, prezygocentrodiapophyseal fossa; prz, prezygapophyses; tp, transverse process. Scale bar equals 50 mm.

Evers *et al.* (2015)]. The centrodiapophyseal lamina runs from the diapophysis, extending from the ventral surface of the transverse process toward the lateral side of the centrum, resulting in a 'T-shaped' cross-section of the transverse process.

Regarding the pneumaticity of the vertebra, the prezygocentrodiapophyseal fossa is open ventrolaterally and extends throughout the anteroventral part of the transverse process (Fig. 13A, B). This fossa is delimited by the centroprezygapophyseal lamina anteriorly, the centrodiapophyseal lamina posteriorly, and the prezygodiapophyseal lamina dorsally. The prezygocentrodiapophyseal fossa presents a 'slit-shaped' foramen, quite high, narrow, and oval, which penetrates the pedicle of the prezygapophysis. The postzygocentrodiapophyseal fossa is located on the posterior surface of the transverse process, being larger than the prezygocentrodiapophyseal fossa (Fig. 13C, D). This fossa is delimited anteriorly by the centrodiapophyseal lamina, posteriorly by the centropostzygapophyseal lamina and dorsally by the postzygodiapophyseal lamina. Moreover, it exhibits another pneumatic foramen, which penetrates posterolaterally into the transverse process, and is also more circular than that of the prezygocentrodiapophyseal fossa (Fig. 13C, D).

The prezygapophyses are large and considerably separated, projecting more laterally than the vertebral centrum itself, being projected mainly dorsolaterally and slightly anteriorly (Fig. 13A–F). The prezygapophyses are located dorsal to the transverse process in the anterior half of the transverse processes and their anterior margin is placed slightly anterior to the anterior margin of the transverse process (Fig. 13I–L). The prezygapophyseal articular facets of the prezygapophyses are oval to subcircular in dorsal view, being wider laterally. They are dorsomedially facing, with an angle of 125° between both facets. These facets are slightly convex but almost flat, and slightly posteriorly inclined. There is no intraprezygapophyseal lamina between the prezygapophyses.

The postzygapophyses are also large, but more compact compared to the prezygapophyses and without an epipophysis. They extend posterodorsally beyond the posterior margin of the centrum, with half of the postzygapophyses posterior to the posterior margin of the centrum (Fig. 13I–L). The postzygapophyseal facets are concave, with an inverted 'teardrop-shape', posteroventrally facing, and laterally oriented. They are connected anteromedially by the spinopostzygapophyseal laminae, but they are not connected ventromedially because there is no intrapostzygapophyseal lamina. Nevertheless, from the posteromedial margin of the postzygapophyses, two narrow spinopostzygapophyseal laminae extend ventrally, reaching the dorsolateral edge of the neural spine. The spinopostzygapophyseal laminae are well developed, robust, and rounded, being delimited dorsolaterally by the spinopostzygapophyseal fossa, which

is quite triangular and open ventrally. This fossa is laterally delimited by postzygapophyses and ventromedially oriented laminae.

The neural spine is not completely preserved, but its base suggests that it was a 'spike-like' process that projected posterodorsally (Fig. 13A–F). The cross-section of its base is subcircular in dorsal view, and is connected to the prezygapophyses by the spinoprezygapophyseal laminae. These laminae are poorly developed in comparison to the other laminae present in the vertebra; besides that, they are rounded and extend from the anterior surface of the neural spine to the posteromedial margin of the prezygapophyses, forming an inverted 'V-shaped' structure (Fig. 13A–F). A prespinal lamina (*sensu* Evers *et al.* 2015) is also present on the anterior surface of the neural arch, situated between the spinoprezygapophyseal laminae. This lamina is low, dorsoventrally oriented, and projects slightly ventrally into the neural canal. This lamina, together with the spinoprezygapophyseal laminae, delimits a shallow triangular depression on the anterior surface of the neural arch.

Morphological comparisons

Specimen NHMUK PV R 38358 shares with many early-branching tetanuran theropods the single pneumatic foramen on the lateral surface of the vertebral centrum (Carrano *et al.* 2012). Furthermore, this posterior cervical vertebra shares with Megalosauroidea taxa the bordered (or rimmed) anterior articular surface of the centrum (Carrano *et al.* 2012, Evers *et al.* 2015, Malafaia *et al.* 2020, Barker *et al.* 2021). However, this trait may be also present in *Allosaurus* (Rauhut and Pol 2019). In the specimen studied here, the parapophyses are enlarged and exhibit a strongly concave facet, similar with the spinosaurids *Baryonyx*, *Ichthyovenator*, *Sigilmassasaurus*, and *Suchomimus* (Allain *et al.* 2012, Evers *et al.* 2015). Another feature shared between NHMUK PV R 38358 and spinosaurids is the presence of a ventral keel on the vertebral centrum, with the anterior end projecting anteriorly (a synapomorphy for Spinosauridae—Schade *et al.* 2023). The neural arch of NHMUK PV R 38358 lacks epipophyses, similar to the posterior cervicals of *Baryonyx* [considering the arrangement proposed by Evers *et al.* (2015)], and *Sigilmassasaurus* (Russell 1996, McFeeters *et al.* 2013, Evers *et al.* 2015). The neural spine is inferred to be 'spike-like' in NHMUK PV R 38358, a feature also shared with *Baryonyx* and *Sigilmassasaurus* (Evers *et al.* 2015).

The vertebral centrum of NHMUK PV R 38358 is very wide, with the anterior articular surface being 1.4 times wider than it is tall, similar to the condition observed in *Ichthyovenator* and *Sigilmassasaurus*, in the latter being more than 1.5 times larger than high (Russell 1996, McFeeters *et al.* 2013, Evers *et al.* 2015). Specimen NHMUK PV R 38358 also shares with *Ichthyovenator* and *Sigilmassasaurus* the lack of intraprezygapophyseal and intrapostzygapophyseal laminae (Allain *et al.* 2012, Evers *et al.* 2015). The posterior cervical vertebra (C9) studied here further resembles the posterior cervicals of *Sigilmassasaurus brevicollis* by having large, transverse processes that exhibit pneumatic foramina deep beneath their base (McFeeters *et al.* 2013, Evers *et al.* 2015).

If the emended diagnosis of *Sigilmassasaurus brevicollis* proposed by Evers *et al.* (2015) is considered, specimen NHMUK PV R 38358 shares with the former the reduced lamination of the neural arch with the centrodiapophyseal laminae not being divided into anterior and posterior centrodiapophyseal laminae [autapomorphy proposed by Evers *et al.* (2015)]. Nevertheless, the specimen described here lacks the anterior tubercle that is present on the anterior articular surfaces of the posterior cervical and anterior dorsal vertebrae of *Sigilmassasaurus brevicollis* (McFeeters *et al.* 2013, Evers *et al.* 2015), but this feature is more subtle in the BSPG 2011 I 115 cervical vertebra (Evers *et al.* 2015) and also absent in ROM 65537 (McFeeters *et al.* 2013). The posterior vertebra NHMUK PV R 38358 can be safely assigned to Spinosauridae, furthermore, due to the above-mentioned features shared with *Sigilmassasaurus brevicollis*, we here assign this specimen to the same taxon.

Allosauroidea Marsh, 1878

Carcharodontosauria Benson *et al.*, 2010

Carcharodontosauridae Stromer, 1931

Carcharodontosauridae gen. et sp. indet.

(Fig. 14)

Referred specimen

A partial left ischium (NHMUK PV R 16437).

Morphological description

The left ischium NHMUK PV R 16437 has its proximal portion preserved, missing the distalmost portion of the shaft and the ventralmost portion of the obturator process (Fig. 14). The iliac and pubic peduncles are separated by a concave acetabular rim that is shallow, wide in anterior view with a middle constriction, giving it an 'hourglass-shape' in proximal view (Fig. 14). The peduncles are subequal in size. In the proximal region, the iliac articular surface is triangular and deeply concave suggesting a peg-and-socket articulation (Fig. 14). In the anteriormost region of the iliac peduncle, anterior to the articular surface with the ilium, the ischium is thick mediolaterally, forming the ischial antitrochanter, which is parallelogram-shaped in anterior view. Although the antitrochanter is thick, it is not well projected, being a reduced ridge. In the posterior part of the iliac joint, there is a posterior flange that rises, and it is broken in the dorsalmost portion. The pubic peduncle is subtriangular and medially concave with the articular surface being laterally oriented.

The lateral and medial surfaces of the ischium are concave between the peduncles, with the concavity displaced dorsally in the lateral side and ventrally in the medial side. Posteroventral to the flange in the iliac peduncle, a deep and rugose sulcus, homologous to the ischial tuberosity (e.g. Hutchinson 2001b, Brusatte *et al.* 2008, Cuesta *et al.* 2018), runs in the lateral surface becoming shallower posteriorly (Fig. 14). The most proximal part of this sulcus, somewhat elliptical in shape, represents the osteological correlate of the origin of the muscle *flexor tibialis internus 3* (FTI3), which is delimited slightly more distally. The most distal part of the sulcus in the posterodorsal region of the ischial shaft, which is more linear, less elliptical than the proximal part, becomes shallower distally, and represents the osteological correlate of the origin of the muscle *adductor femoris 2* (ADD2) (Fig. 14A, B). Both of these muscle origins are level II inferences

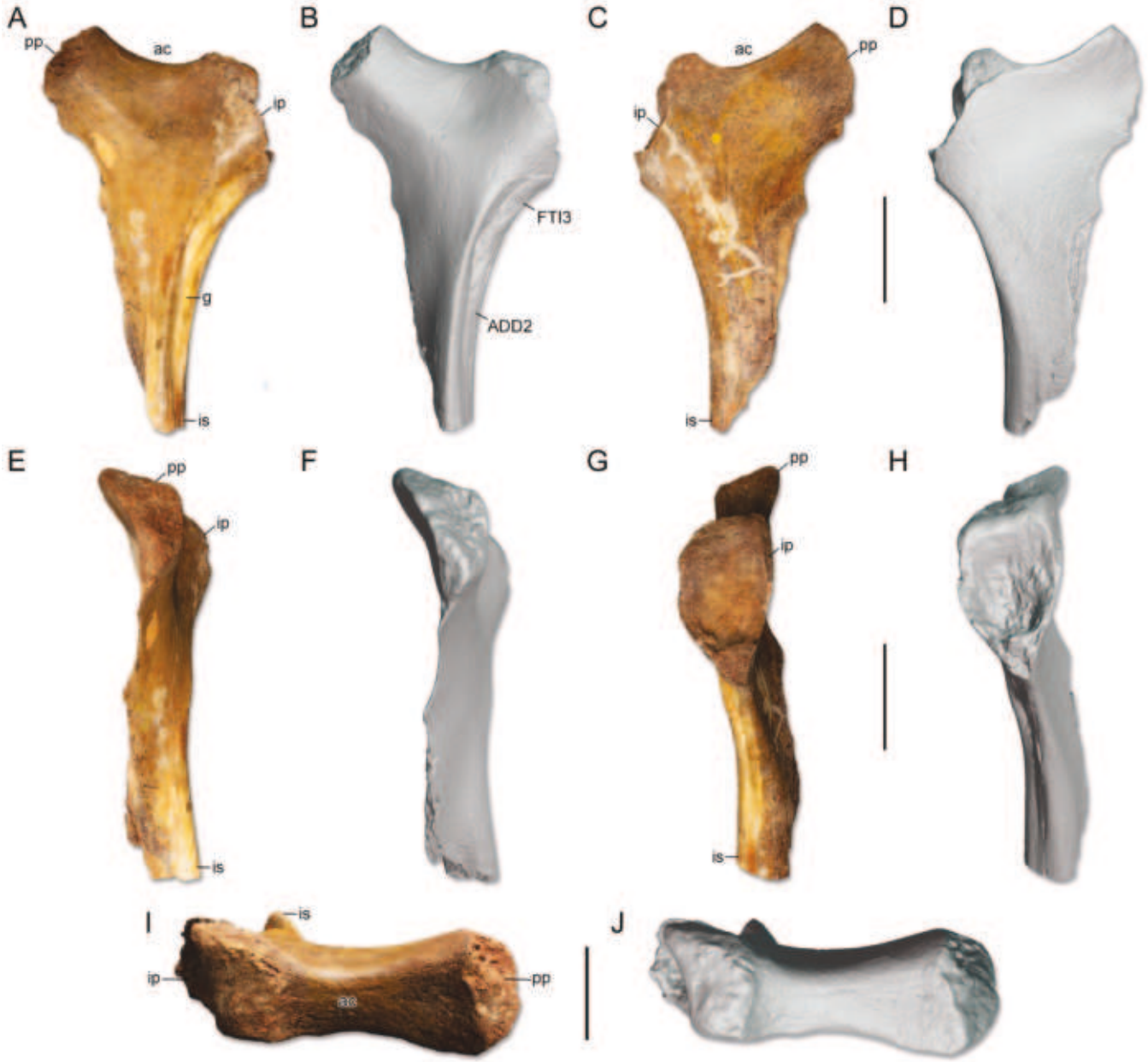

Figure 14. Ischium of Carcharodontosauridae indet. NHMUK PV R 16437. A, B, left lateral; C, D, medial; E, F, anterior; G, H, posterior; and I, J, proximal views. Anatomical abbreviations: ac, acetabulum; ADD2, *M. adductor femoris 2* origin scar; FTI3, *M. flexor tibialis internus 3* origin scar; g, groove; ip, iliac peduncle; is, ischial shaft; pp, pubic peduncle. Scale bar equals 100 mm (A–H) and 40 mm (I–J).

by Witmer's (1995) systematization and are topologically compatible with other theropods (e.g. ceratosaurs—Cerroni *et al.* 2024, early tetanurans—Lacerda *et al.* 2024, and derived coelurosaurs—Carrano and Hutchinson 2002).

In the preserved portion of the ischium, the shaft is dorsoventrally flattened, giving it a subrectangular shape, lacking the distalmost part (Fig. 14). Ventral to the shaft and posterior to the pubic peduncle, the obturator process is separated from the pubic peduncle by a shallow and anteroposteriorly notch. Posterior to this notch, the obturator process is twisted medially from the pubic peduncle and broken in its ventralmost portion (however, a notch ventral to obturator process can be noted) and seems to be confluent with the shaft (Fig. 14). Although the ischial shaft is not completely preserved, the preserved part is straight, suggesting that the orientation of the main axis of the ischium was straight in NHMUK PV R 16437.

Morphological comparisons

The overall shape of the NHMUK PV R 16437 partial ischium resembles that of carcharodontosaurid theropods rather than of other dinosaurs. The acetabular rim is shallow in lateral view with a weak 'U-shape' due to the ventral position of the pubic peduncle, as seen in allosauroids (*sensu* Rauhut and Pol 2019), including the carcharodontosaurids *Acrocanthosaurus*, *Concavenator*, *Giganotosaurus*, *Mapusaurus*, and *Neovenator*. In some neovenatorids, such as *Siats*, the acetabular rim is shallow,

not forming a 'U-shaped' border, being straighter than in other allosauroids (Zanno and Makovicky 2013). The 'U-shape' of the acetabular rim is more pronounced in megalosauroids such as *Piatnitzkysaurus* and also in the spinosaurids *Baryonyx*, *Ichthyovenator*, *Vallibonavenatrix*, FSAC-KK 11888, and possibly in *Suchomimus* due to a dorsal projection of the pubic peduncle (Allain *et al.* 2012, Malafaia *et al.* 2020, Sereno *et al.* 2022, Lacerda *et al.* 2024). This condition differs from that observed in NHMUK PV R 16437.

The ilioischiatic articulation of NHMUK PV R 16437 has a deep peg-and-socket (or ball-and-socket) configuration, as seen in *Acrocanthosaurus*, *Concavenator*, *Giganotosaurus*, *Mapusaurus*, and *Siats* (Stovall and Langston 1950, Coria and Currie 2006, Carrano *et al.* 2012, Zanno and Makovicky 2013, Cuesta *et al.* 2018, Rauhut and Pol 2019, Lacerda *et al.* 2023). In other theropods, this articulation has a concave plane configuration (e.g. Carrano *et al.* 2012, Lacerda *et al.* 2023, Isasmendi *et al.* 2024).

The ischial antitrochanter is a well-developed, notch-shaped structure in coelophysoids, some ceratosaurs, the early tetanuran *Sinosaurus*, the spinosaurid *Ichthyovenator*, and the neovenatorid *Siats*; it is a reduced notch in the ischium of other theropods (e.g. Allain *et al.* 2012, Carrano *et al.* 2012, Zanno and Makovicky 2013, Cuesta *et al.* 2018, Lacerda *et al.* 2023). In NHMUK PV R 16437, although the ischial antitrochanter is a reduced ridge, it represents a thick structure at its base, and this is more comparable with forms such as *Acrocanthosaurus*, *Giganotosaurus*, and *Sinraptor*, than *Siats* and other contemporary theropods such as spinosaurids.

The presence of the sulcus in the dorsolateral shaft of the ischium, which is posterior to the flange, is similar in NHMUK PV R 16437 and other theropods (e.g. Zanno and Makovicky 2013, Cuesta *et al.* 2018); however, in the ischium described here it is deeper, similar to carcharodontosaurids and neovenatorids rather than spinosaurids. Consequently, the osteological correlates of the origins of the muscles FTI3 (proximal) and ADD2 (distal) in NHMUK PV R 16437 are deeper than those noted in other non-carcharodontosaurid theropods (e.g. Carrano and Hutchinson 2002, Cerroni *et al.* 2024, Lacerda *et al.* 2024).

The obturator process of NHMUK PV R 16437 presents a notch that is shared with other theropods such as the ceratosaur *Ceratosaurus*, piatnitzkysaurids, spinosaurids (except *Ichthyovenator*), and allosauroids such as *Acrocanthosaurus*, *Allosaurus*, *Giganotosaurus*, and *Sinraptor* (Stovall and Langston 1950, Carrano *et al.* 2012, Lacerda *et al.* 2023). However, NHMUK PV R 16437 has a lamina, part of the dorsalmost portion of the obturator process, which is immediately ventral to the pubic peduncle. This feature is also shared with the metriacanthosaurid *Sinraptor* and the carcharodontosaurid *Giganotosaurus*.

Furthermore, if the ischial shaft in NHMUK PV R 16437 is indeed straight, as the preserved portion suggests, this would be another feature shared between this individual and carcharodontosaurids (also seem in some allosauroids—Madsen 1976), but not with some early diverging tetanurans and also metriacanthosaurids. Thus, based on the set of characteristics shared between NHMUK PV R 16437 and carcharodontosaurid theropods, as well as the differences between this ischium and those of spinosaurids, we assign this material to an indeterminate Carcharodontosauridae.

Brief survey of theropod dinosaurs from the Kem Kem Group

Several records of theropod dinosaurs are known from the North Africa, especially those that derive from Middle Cretaceous rocks from the Kem Kem Group region, therefore, suggesting a high theropod diversity. However, much of the diversity known for the region is represented by shed teeth, which are more likely to be fossilized as they are more resistant to weathering and taphonomic alterations (Benyoucef *et al.* 2015, Hendrickx *et al.* 2024). There is also a good and broad ichnological record that helps confirm faunal occurrences and serves as a proxy for more reliable palaeoenvironmental reconstructions (Belvedere *et al.* 2013, Ibrahim *et al.* 2014b). Regarding skeletal remains, records are scarcer (Hendrickx *et al.* 2024); however, they are still of broad relevance for understanding both biogeographical and evolutionary issues in different clades. Below, a brief non-exhaustive survey of the body fossil occurrences is presented, as well as integration with our findings and their relevance to current knowledge.

Abelisauridae

The fossil record of abelisaurids is one of the most abundant in the Kem Kem Group, being less abundant only than spinosaurids. Russell (1996) described several bone fragments, including two partial right dentaries, in addition to two partial cervical vertebrae that were attributed to an undetermined theropod, but recently were assigned to abelisaurids (Souza-Júnior *et al.* 2023). Although the locality from which these materials were derived is unknown, they were probably recovered from the Cenomanian of southern Morocco (Souza-Júnior *et al.* 2023). A partially preserved maxilla that probably comes from Erfoud was described by Mahler (2005). Novas *et al.* (2005) related a ungual pedal to Abelisauroidea from the Tafilalt region. A partially preserved left maxilla that derives from a region near Taouz was described by Porchetti *et al.* (2011). The proximal part of a femur was described by Chiarenza and Cau (2016). In addition to these, an axis vertebra described by Smyth *et al.* (2020a) was also attributed to Abelisauridae.

Noasauridae

A postcranial skeleton that is relatively well preserved, including hindlimbs and partial forelimbs as well as part of the tail, was erected as *Deltradomeus agilis* by Sereno *et al.* (1996). However, the assignment of this taxon to noasaurid theropods occurred only in later phylogenetic analyses (e.g. Sereno *et al.* 2004) and the phylogenetic position of this taxon remains under debate. Evans *et al.* (2015) described a well-preserved femur from south-east Taouz, which could possibly belong to *Deltradomeus*. Another noasaurid occurrence was presented by Smyth *et al.* (2020a), based on an isolated cervical vertebra.

Spinosauridae

This group is one of the most representative in the Kem Kem Group fossil record; however, the nature of the material is isolated or semi-articulated fossils. Two partial dentaries from south-eastern Morocco were described by Buffetaut (1989), being both referred to *Spinosaurus* cf. *Sp. aegyptiacus*. Based on a set of isolated bones, including cervical vertebrae, dorsal neural arch, and a fragmentary dentary recovered from Morocco,

Russell (1996) erected the name *Spinosaurus maroccanus*; later on, Taquet and Russell (1998) referred a rostrum and some axial elements recovered from the Algerian portion of the Sahara Desert to this species. However, this species is frequently regarded as a *nomen dubium* (e.g. Carrano *et al.* 2012), a junior synonym of *Spinosaurus aegyptiacus* (e.g. Ibrahim *et al.* 2014a), or Spinosaurinae indet. (e.g. Lacerda *et al.* 2022). Milner (2003) presented a rostrum and a relatively well-preserved dentary from Morocco in a brief note; both of them were referred to *Sp. aegyptiacus*. This rostrum is redescribed in detail in this work (NHMUK PV R 16420) and considered as an indeterminate Spinosaurinae, agreeing with the current debate (e.g. Sales and Schultz 2017, Lacerda *et al.* 2022). Another rostrum, which represents the most complete and well-preserved known to date, and a pair of nasals from Morocco were described by Dal Sasso *et al.* (2005), with both referred to *Spinosaurus* cf. *Sp. aegyptiacus*. Lately, some studies (e.g. Sales and Schultz 2017, Lakin and Longrich 2019, Lacerda *et al.* 2022) have argued that the most reliable identification of that rostrum is Spinosaurinae indet. due to a lack of overlap between these specimens and the *Sp. aegyptiacus* holotype. Based on several skeletal elements of a subadult individual, Ibrahim *et al.* (2014a) proposed a neotype to *Sp. aegyptiacus*, and later on, new skeletal remains possibly of the same individual represented by a robust tail were also recovered from Morocco (Ibrahim *et al.* 2020a). Two morphotypes of spinosaurids, *Sp. aegyptiacus* and cf. *Sigilmassasaurus brevicollis*, were identified by Hendrickx *et al.* (2016) based on six quadrates that probably derived from Morocco. A tiny pedal ungual recovered from between the villages of Taouz and Begaa was presented by Maganuco and Dal Sasso (2018). Arden *et al.* (2019) also described two morphotypes of spinosaurids from the Kem Kem Group: one referred to *Sp.* cf. *Sp. aegyptiacus* based on frontals and a frontoparietal, and a skull roof referred to *Sigilmassasaurus* cf. *Si. brevicollis*. Based on cranial remains and isolated axial elements, Lakin and Longrich (2019) also described fossils referred to *Si. brevicollis* and *Sp.* cf. *Sp. aegyptiacus*. Besides the previous mentions, other studies also described axial elements of *Sigilmassasaurus brevicollis* recovered from the same region (e.g. Russell 1996, McFeeters *et al.* 2013, Evers *et al.* 2015).

In this contribution we have described several specimens that expand the knowledge of occurrences of spinosaurids in the Kem Kem Group. Among these, we have presented a cervical vertebra referred to *Si. brevicollis* (NHMUK PV R 38358), in addition to nine specimens (NHMUK PV R 16391, 16422, 16423, 16424, 16426, 16430, 16431, 16433, 16438) that we conservatively classified as indeterminate Spinosaurinae. Our findings, combined with materials mentioned above, contribute to general aspects of the occurrence of spinosaurids in the region, making them one of the most abundant groups of theropod dinosaurs in the Kem Kem Group.

Carcharodontosauridae

At least two species are known from the Kem Kem Group (although some studies consider only one species—Ibrahim *et al.* 2020a). A nearly complete skull and some vertebral elements of *Carcharodontosaurus saharicus* were described by Sereno *et al.* (1996), in which a neotype was designated, recovered from the Douira Formation, south-eastern Morocco (Sereno *et al.* 1996, Ibrahim *et al.* 2020a). An isolated and fragmentary portion of a dentary [originally referred to an abelisaurid by Russell (1996)—see Ibrahim *et al.* (2020a)] can also be assigned to *C. saharicus*. A second carcharodontosaurid species, *Sauroniops pachytholus*, was erected by Cau *et al.* (2013) based on an almost complete frontal. Later on, Paterna and Cau (2023) also referred additional materials (a partial maxilla and a jugal) to Carcharodontosauridae, discussing the status of both—*Carcharodontosaurus* and *Sauroniops*. A probably indeterminate carcharodontosaurids manual ungual [Ibrahim *et al.* (2020a), originally described as Theropoda indet. by Russell (1996)] adds to the fossil record of this clade.

Here we also provided the description of an isolated ischium we identify as an indeterminate carcharodontosaurid (NHMUK PV R 16437), adding to the fossil record of this clade from the Kem Kem Group.

Taxonomic attributions of NHMUK PV R 16420 and MSNM V4047 snouts

There is a consensus in the literature considering both well-preserved rostra from the Kem Kem Group—NHMUK PV R 16420 and MSNM V4047—as Spinosaurinae theropods (e.g. Milner 2003, Dal Sasso *et al.* 2005, Lakin and Longrich 2019, Lacerda *et al.* 2022). However, the referral of both to *Spinosaurus aegyptiacus* (e.g. Milner 2003, Dal Sasso *et al.* 2005, Ibrahim *et al.* 2014a) is not possible to corroborate, at least yet, due to the lack of overlap among these and the *Sp. aegyptiacus* holotype (Evers *et al.* 2015, Sales and Schultz 2017, Lakin and Longrich 2019, Lacerda *et al.* 2022).

Some studies (Lakin and Longrich 2019, Lacerda *et al.* 2022) noted some differences between both specimens. Lakin and Longrich (2019) considered NHMUK PV R 16420 as having a deeply concave dorsal profile and a curved premaxillary ventral profile, a straighter maxillary tooth row, larger external nares, and distinct outline of the premaxilla when compared with MSNM V4047. Although Lakin and Longrich (2019) did not consider these, necessarily, as two distinct taxa, they considered this set of features enough to designate two distinct morphotypes. However, Lacerda *et al.* (2022) quantitatively showed a high degree of compression/erosion in NHMUK PV R 16420, preventing any morphological differentiation from MSNM V4047.

As previous noted, the only major differences between the two rostra are the number of premaxillary teeth and the pattern of the intramaxillary suture anteriorly. However, these features seem to have no systematic significance. Based on our detailed redescription, we reject the possibility of two distinct taxa based on the NHMUK PV R 16420 and MSNM V4047 rostra. Excluding some features that are taphonomic artefacts, both snouts have virtually the same shape and probably represent the same taxon.

One or two Spinosaurinae taxa in the Kem Kem Group?

There is a prolific debate regarding the presence of one or more spinosaurid species in the Cenomanian of the Kem Kem Group. Several studies consider that *Spinosaurus aegyptiacus* is the only well-established species from this region and *Sigilmassasaurus*

brevicollis is not supported due to the lack of autapomorphies (e.g. Ibrahim *et al.* 2014a, 2020a, b, Maganuco and Dal Sasso 2018, Smyth *et al.* 2020b). Meanwhile, other studies have argued the plausibility of two (contemporary?) species, considering *Si. brevicollis* a valid taxon (McFeeters *et al.* 2013, Evers *et al.* 2015, Hendrickx *et al.* 2016, Hone and Holtz 2017, Arden *et al.* 2019). However, there is a degree of plausibility to both propositions, as we explain here. On one hand, those studies that consider *Sp. aegyptiacus* the only species argue that any morphological variation noted in multiple specimens is due to ontogeny, individual variations or sexual dimorphism (e.g. Ibrahim *et al.* 2014b, Smyth *et al.* 2020b). Nevertheless, there are no studies showing the main ontogenetic stages of *Sp. aegyptiacus*, for example, leaving these propositions as speculative. On the other hand, several 'diagnostic' or 'autapomorphic' features are described in the literature, and several studies discuss distinct morphotypes of spinosaurids from the Kem Kem Group (e.g. Chiarenza and Cau 2016, Hendrickx *et al.* 2016, Arden *et al.* 2019; McFeeters 2021).

This study also supports different morphotypes from this geological unit, for example, based on the proximal portion of the femur described here (NHMUK PV R 16433) when compared with the proximal femur attributed to *Sp. aegyptiacus* (FSAC-KK 11888; Ibrahim *et al.* 2014a, Sereno *et al.* 2022). Besides that, several fossil specimens that have been synonymized with, and referred to, *Sp. aegyptiacus* do not even overlap with the lost holotype specimen (Evers *et al.* 2015, Sales and Schultz 2017, Lakin and Longrich 2019, Lacerda *et al.* 2022), and thus remain difficult to corroborate. Although this study does not intend to resolve these issues, we considered the extended diagnosis provided by Evers *et al.* (2015), and thus the potential validity of *Si. brevicollis*. Meanwhile, we did not relate other materials to *Sp. aegyptiacus* due to lack of overlap and the possibility of a proper morphological comparison. Our study highlights the complexity of the analysis of spinosaurid diversity from the Kem Kem Group, and describes some fossil remains in detail, instead of only mentioning the occurrences of fossils, lacking proper descriptions and anatomical comparisons. We urge a detailed review of all spinosaurid materials from the Kem Kem Group, and also suggest caution in considering either a single taxon of spinosaurine with a large amount of morphological variation, or two taxa lacking proper diagnosis; thus, encouraging more detailed/rigorous studies. Resolution of this issue probably depends upon new discoveries of specimens.

CONCLUSION

As more spinosaurid material is discovered in the Cenomanian layers of the Kem Kem Group, aspects about the morphology and diversity of this clade continue to increase. Here we present 11 new specimens, including indeterminate spinosaurines, *Sigilmassasaurus*, and a specimen of an indeterminate carcharodontosaurid. In addition to these, a detailed redescription of a well-preserved spinosaurine snout is provided. Among the Spinosaurinae finds, an isolated femur from a juvenile individual suggests a strong and robust caudal muscle (*M. caudofemoralis longus*) based on its osteological correlates. Our study highlights the complexity of analysing the diversity of spinosaurids from the Kem Kem Group, which is one of the most abundant theropod clades in the fossil record from this unit. We support different morphotypes and our study encourages a detailed review of all spinosaurid materials from the Kem Kem Group.

ACKNOWLEDGMENTS

We are profoundly grateful to the curators who gave us access to materials under their care: Marc Jones (NHMUK), Michael Day (NHMUK), Susannah Maidment (NHMUK), Luciana Carvalho (MN/UFRJ), Orlando Grillo (MN/UFRJ), and Eliza Howlett (OUMNH). We also thank MorphoSource for storing the 3D digital models (projects: UCRC:PV170 and UCRC:PV171) used in the comparisons, which were provided by Stephanie Baumgart (University of Chicago), and for representing a repository in which we insert 3D digital models of the materials described here. We also acknowledge Cristiano Dal Sasso (MSNM) for providing photos of the MSNM V6900 specimen, Simone Maganuco (MSNM) and Bruno Navarro (USP) for sharing information/literature useful for this study, and Camila Pinto (IFSC/USP), Masaya Iijima (IVPP) and Yuting Lin (RVC) for comments and assistance provided throughout this research; Masaya is also thanked for his assistance during the digitization of the specimens. We are especially grateful to Associate Editor Eduardo Puértolas Pascual and to the comments made by Elisabete Malafaia and an anonymous referee, improving the clarity of the manuscript.

CONFLICT OF INTEREST

None declared.

FUNDING

This work was partially supported by the Coordenação de Aperfeiçoamento de Pessoal de Nível Superior (CAPES 88882.461737/2019-01, to M.B.S.L.), Conselho Nacional de Desenvolvimento Científico e Tecnológico (CNPq 200203/2022-3, to M.B.S.L.), Spanish Ministry of Science, Innovation and Universities and the European Regional Development Fund (CGL2017-85038-P and PID2021-122612OB-I00, MINECO/FEDER, UE, to E.I.), the Basque Government/Eusko Jaurlaritza (research groups IT418-19, IT1485-22, and PRE_2019_1_0215, to E.I.), the University of the Basque Country (UPV/EHU, group PPG17/05, to E.I.), Fundação de Amparo à Pesquisa do Estado de São Paulo (FAPESP 2020/07997-4; 2022/14375-5, to R.D.) and European Research Council Horizon 2020 Advanced Investigator Grant (ERC 695517, to J.R.H.).

DATA AVAILABILITY

All 3D digital models generated by this study are included and figured in the manuscript and have been deposited in MorphoSource (Project ID 000623669 [https://www.morphosource.org/projects/000623669])

REFERENCES

Allain R, Tykoski R, Aquesbi N *et al.* An abelisauroid (Dinosauria: Theropoda) from the Early Jurassic of the High Atlas Mountains, Morocco, and the radiation of ceratosaurs. *Journal of Vertebrate Paleontology* 2007;**27**:610–24. https://doi.org/10.1671/0272-4634(2007)27[610:aadtft]2.0.co;2

Allain R, Xaisanavong T, Richir P *et al.* The first definitive Asian spinosaurid (Dinosauria: Theropoda) from the early Cretaceous of Laos. *Naturwissenschaften* 2012;**99**:369–77. https://doi.org/10.1007/s00114-012-0911-7

Alloul T, Rage JC, Hamdidouche R *et al.* First report on Cretaceous vertebrates from the Algerian Kem Kem beds. A new procoelous salamander from the Cenomanian, with remarks on African Caudata. *Cretaceous Research* 2018;**84**:384–8. https://doi.org/10.1016/j.cretres.2017.11.019

Alonso A, Canudo JI. On the spinosaurid theropod teeth from the early Barremian (Early Cretaceous) Blesa Formation (Spain). *Historical Biology* 2016;**28**:823–34. https://doi.org/10.1080/08912963.2015.1036751

Alonso A, Canudo JI, Fernández-Baldor FT *et al.* Isolated theropod teeth associated with sauropod remains from El Oterillo II (Early Cretaceous) site of Salas de los Infantes (Burgos, Spain). *Journal of Iberian Geology* 2017;**43**:193–215. https://doi.org/10.1007/s41513-017-0017-3

Alonso A, Gasca JM, Navarro-Lorbés P *et al.* A new contribution to our knowledge of the large-bodied theropods from the Barremian of the Iberian Peninsula: the 'Barranco del Hocino' site (Spain). *Journal of Iberian Geology* 2018;**44**:7–23. https://doi.org/10.1007/s41513-018-0051-9

Amiot R, Buffetaut E, Tong H *et al.* Isolated theropod teeth from the Cenomanian of Morocco and their palaeobiogeographical significance. *Revue de Paléobiologie* 2004;**9**:143–9.

Arden TMS, Klein CG, Zouhri S *et al.* Aquatic adaptation in the skull of carnivorous dinosaurs (Theropoda: Spinosauridae) and the evolution of aquatic habits in spinosaurids. *Cretaceous Research* 2019;**93**:275–84. https://doi.org/10.1016/j.cretres.2018.06.013

Barker CT, Hone DW, Naish D *et al.* New spinosaurids from the Wessex Formation (Early Cretaceous, UK) and the European origins of Spinosauridae. *Scientific Reports* 2021;**11**:19340. https://doi.org/10.1038/s41598-021-97870-8

Baumel JJ, Witmer LM. Osteologia. In Baumel JJ, King AS, Breazile JE, Evans HE, Vanden Berge JC (eds), *Handbook of Avian Anatomy: Nomina Anatomica Avium*, 2nd edn. Cambridge, MA: Publications of the Nutall Ornithological Club, 1993, 45–132.

Belvedere M, Jalil NE, Breda A *et al.* Vertebrate footprints from the Kem Kem beds (Morocco): a novel ichnological approach to faunal reconstruction. *Palaeogeography, Palaeoclimatology, Palaeoecology* 2013;**383-384**:52–8. https://doi.org/10.1016/j.palaeo.2013.04.026

Benson RB. A description of *Megalosaurus bucklandii* (Dinosauria: Theropoda) from the Bathonian of the UK and the relationships of Middle Jurassic theropods. *Zoological Journal of the Linnean Society* 2010;**158**:882–935. https://doi.org/10.1111/j.1096-3642.2009.00569.x

Benson RB, Carrano MT, Brusatte SL. A new clade of archaic large-bodied predatory dinosaurs (Theropoda: Allosauroidea) that survived to the latest Mesozoic. *Naturwissenschaften* 2010;**97**:71–8. https://doi.org/10.1007/s00114-009-0614-x

Benyoucef M, Läng E, Cavin L *et al.* Overabundance of piscivorous dinosaurs (Theropoda: Spinosauridae) in the mid-Cretaceous of North Africa: the Algerian dilemma. *Cretaceous Research* 2015;**55**:44–55. https://doi.org/10.1016/j.cretres.2015.02.002

Brusatte S, Benson R, Hutt S. The osteology of *Neovenator salerii* (Dinosauria: Theropoda) from the Wealden Group (Barremian) of the Isle of Wight. *Monograph of the Palaeontographical Society Series* 2008;**162**:1–75.

Buffetaut E. New remains of the enigmatic dinosaur *Spinosaurus* from the Cretaceous of Morocco and the affinities between *Spinosaurus* and *Baryonyx*. *Neues Jahrbuch für Geologie und Paläontologie. Monatshefte* 1989;**1989**:79–87. https://doi.org/10.1127/njgpm/1989/1989/79

Bunker G, Martill DM, Smith RE *et al.* Plesiosaurs from the fluvial Kem Kem Group (mid-Cretaceous) of eastern Morocco and a review of non-marine plesiosaurs. *Cretaceous Research* 2022;**140**:105310. https://doi.org/10.1016/j.cretres.2022.105310

Canale JI, Apesteguía S, Gallina PA *et al.* New giant carnivorous dinosaur reveals convergent evolutionary trends in theropod arm reduction. *Current Biology: CB* 2022;**32**:3195–202.e5. https://doi.org/10.1016/j.cub.2022.05.057

Canudo JI, Gasulla JM, Gómez-Fernández D *et al.* Primera evidencia de dientes aislados atribuidos a Spinosauridae (Theropoda) en el Aptiano inferior (Cretácico Inferior) de Europa: formación Arcillas de Morella (España). *Ameghiniana* 2008;**45**:649–52.

Carrano MT, Hutchinson JR. Pelvic and hindlimb musculature of *Tyrannosaurus rex* (Dinosauria: Theropoda). *Journal of Morphology* 2002;**253**:207–28. https://doi.org/10.1002/jmor.10018

Carrano MT, Benson RB, Sampson SD. The phylogeny of Tetanurae (Dinosauria: Theropoda). *Journal of Systematic Palaeontology* 2012;**10**:211–300. https://doi.org/10.1080/14772019.2011.630927

Cau A, Dalla Vecchia FM, Fabbri M. A thick-skulled theropod (Dinosauria, Saurischia) from the Upper Cretaceous of Morocco with implications for carcharodontosaurid cranial evolution. *Cretaceous Research* 2013;**40**:251–60. https://doi.org/10.1016/j.cretres.2012.09.002.

Cavin L, Tong H, Boudad L *et al.* Vertebrate assemblages from the early Late Cretaceous of south-eastern Morocco: *an overview*. *Journal of African Earth Sciences* 2010;**57**:391–412. https://doi.org/10.1016/j.jafrearsci.2009.12.007

Cerroni MA, Canale JI, Novas FE. The skull of *Carnotaurus sastrei* Bonaparte 1985 revisited: insights from craniofacial bones, palate and lower jaw. *Historical Biology* 2021;**33**:2444–85.

Cerroni MA, Otero A, Novas FE. Appendicular myology of *Skorpiovenator bustingorryi*:A first attempt to reconstruct pelvic and hindlimb musculature in an abelisaurid theropod. *The Anatomical Record* 2024. https://doi.org/10.1002/ar.25532

Charig AJ, Milner AC. *Baryonyx walkeri*, a fish-eating dinosaur from the Wealden of Surrey. *Bulletin of the Natural History Museum (Geology)* 1997;**53**:11–70.

Chiarenza AA, Cau A. A large abelisaurid (Dinosauria, Theropoda) from Morocco and comments on the Cenomanian theropods from North Africa. *PeerJ* 2016;**4**:e1754. https://doi.org/10.7717/peerj.1754

Choubert G. Essai sur la paléogéographie du Mésocrétacé marocain. *Société des Sciences Naturelles du Maroc* 1948;**1920210**:307–29.

Coria RA, Currie PJ. A new carcharodontosaurid (Dinosauria, Theropoda) from the Upper Cretaceous of Argentina. *Geodiversitas* 2006;**28**:71–118.

Cuesta E, Ortega F, Sanz JL. Appendicular osteology of *Concavenator corcovatus* (Theropoda: Carcharodontosauridae) from the Lower Cretaceous of Spain. *Journal of Vertebrate Paleontology* 2018;**38**:1–24. https://doi.org/10.1080/02724634.2018.1485153

Currie PJ. Bird-like characteristics of the jaws and teeth of troodontid theropods (Dinosauria, Saurischia). *Journal of Vertebrate Paleontology* 1987;**7**:72–81. https://doi.org/10.1080/02724634.1987.10011638

Dal Sasso C, Maganuco S, Buffetaut E *et al.* New information on the skull of the enigmatic theropod *Spinosaurus*, with remarks on its size and affinities. *Journal of Vertebrate Paleontology* 2005;**25**:888–96. https://doi.org/10.1671/0272-4634(2005)025[0888:NIOTSO]2.0.CO;2

Delfaud J, Zellouf K. Existence, durant le Jurassique et le Crétacé inférieur d'un paléo-Niger coulant du Sud vers le Nord au Sahara occidental. *Bassins Sedimentaires Africains* 1995;**118**:93–104.

Essafraoui B, Ferry S, Groshény D *et al.* Sequence stratigraphic architecture of marine to fluvial deposits across a passive margin (Cenomanian, Atlantic margin, Morocco, Agadir transect). *Carnets de Géologie (Notebooks on Geology)* 2015;**15**:137–72. https://doi.org/10.4267/2042/56909

Evans DC, Barrett PM, Brink KS *et al.* Osteology and bone microstructure of new, small theropod dinosaur material from the early Late Cretaceous of Morocco. *Gondwana Research* 2015;**27**:1034–41. https://doi.org/10.1016/j.gr.2014.03.016

Evers SW, Rauhut OWM, Milner AC *et al.* A reappraisal of the morphology and systematic position of the theropod dinosaur *Sigilmassasaurus* from the 'middle' Cretaceous of Morocco. *PeerJ* 2015;**3**:e1323. https://doi.org/10.7717/peerj.1323

Ferrandini M, Philip J, Babinot J-F *et al.* La plate-forme carbonatée du Cénomano-Turonien de la région d'Erfoud-Errachidia (Sud-Est marocain): stratigraphie et paléoenvironnements. *Bullettin de la Société Géologique de France* 1985;**8**:559–64.

Fitzinger L. *Systema Reptilium. Fasciculus Primus. Amblyglossae*. Vienna: Apud Braumüller and Seidel Bibliopolas, 1843.

Gaffney ES, Tong H, Meylan PA. *Galianemys*, a new side-necked turtle (Pelomedusoides: Bothremydidae) from the Late Cretaceous of

Morocco. *American Museum Novitates* 2002;**3379**:1–20. https://doi.org/10.1206/0003-0082(2002)379<0001:gansnt>2.0.co;2
Gatesy SM. Caudofemoral musculature and the evolution of theropod locomotion. *Paleobiology* 1990;**16**:170–86. https://doi.org/10.1017/s0094837300009866
Gauthier JA. Saurischian monophyly and the origin of birds. In: Padian K (eds), *The Origin of Birds and the Evolution of Flight*. Memoirs of the California Academy of Sciences 1986, **8**, 1–55.
Guiraud R, Bosworth W, Thierry J *et al.* Phanerozoic geological evolution of Northern and Central Africa: an overview. *Journal of African Earth Sciences* 2005;**43**:83–143. https://doi.org/10.1016/j.jafrearsci.2005.07.017
Hassler A, Martin JE, Amiot R *et al.* Calcium isotopes offer clues on resource partitioning among Cretaceous predatory dinosaurs. *Proceedings of the Royal Society B: Biological Sciences* 2018;**285**:20180197. https://doi.org/10.1098/rspb.2018.0197
Hendrickx C, Mateus O. *Torvosaurus gurneyi* n. sp., the largest terrestrial predator from Europe, and a proposed terminology of the maxilla anatomy in nonavian theropods. *PLoS One* 2014;**9**:e88905. https://doi.org/10.1371/journal.pone.0088905
Hendrickx C, Mateus O, Araújo R. A proposed terminology of theropod teeth (Dinosauria, Saurischia). *Journal of Vertebrate Paleontology* 2015;**35**:e982797. https://doi.org/10.1080/02724634.2015.982797
Hendrickx C, Mateus O, Buffetaut E. Morphofunctional analysis of the quadrate of Spinosauridae (Dinosauria: Theropoda) and the presence of *Spinosaurus* and a second spinosaurine taxon in the Cenomanian of North Africa. *PLoS One* 2016;**11**:e0144695. https://doi.org/10.1371/journal.pone.0144695
Hendrickx C, Mateus O, Araújo R *et al.* The distribution of dental features in non-avian theropod dinosaurs: Taxonomic potential, degree of homoplasy, and major evolutionary trends. *Palaeontologia Electronica* 2019;**22.3.74**:1–110. https://doi.org/10.26879/820
Hendrickx C, Trapman TH, Wills S *et al.* A combined approach to identify isolated theropod teeth from the Cenomanian Kem Kem Group of Morocco: cladistic, discriminant, and machine learning analyses. *Journal of Vertebrate Paleontology* 2024:e2311791. https://doi.org/10.1080/02724634.2024.2311791
Hone DWE, Holtz TR Jr. A century of spinosaurs—a review and revision of the Spinosauridae with comments on their ecology. *Acta Geologica Sinica* 2017;**91**:1120–32.
Hutchinson JR. The evolution of femoral osteology and soft tissues on the line to extant birds (Neornithes). *Zoological Journal of the Linnean Society* 2001a;**131**:169–97. https://doi.org/10.1111/j.1096-3642.2001.tb01314.x
Hutchinson JR. The evolution of pelvic osteology and soft tissues on the line to extant birds (Neornithes). *Zoological Journal of the Linnean Society* 2001b;**131**:123–68. https://doi.org/10.1111/j.1096-3642.2001.tb01313.x
Ibrahim N, Sereno PC, Dal Sasso C *et al.* Semiaquatic adaptations in a giant predatory dinosaur. *Science* 2014a;**345**:1613–6. https://doi.org/10.1126/science.1258750
Ibrahim N, Varricchio DJ, Sereno PC *et al.* Dinosaur footprints and other ichnofauna from the Cretaceous Kem Kem Beds of Morocco. *PLoS One* 2014b;**9**:e90751. https://doi.org/10.1371/journal.pone.0090751
Ibrahim N, Maganuco S, Dal Sasso C *et al.* Tail-propelled aquatic locomotion in a theropod dinosaur. *Nature* 2020a;**581**:67–70. https://doi.org/10.1038/s41586-020-2190-3
Ibrahim N, Sereno PC, Varricchio DJ *et al.* Geology and paleontology of the Upper Cretaceous Kem Kem group of eastern Morocco. *ZooKeys* 2020b;**928**:1–216. https://doi.org/10.3897/zookeys.928.47517
Isasmendi E, Navarro-Lorbés P, Sáez-Benito P *et al.* New contributions to the skull anatomy of spinosaurid theropods: Baryonychinae maxilla from the Early Cretaceous of Igea (La Rioja, Spain). *Historical Biology* 2023;**35**:909–23. https://doi.org/10.1080/08912963.2022.2069019
Isasmendi E, Cuesta E, Díaz-Martínez I *et al.* Increasing the theropod record of Europe: a new basal spinosaurid from the Enciso Group of the Cameros Basin (La Rioja, Spain). evolutionary implications and palaeobiodiversity. *Zoological Journal of the Linnean Society* 2024:zlad193. https://doi.org/10.1093/zoolinnean/zlad193
Kellner AW, Azevedo SA, Machado EB *et al.* A new dinosaur (Theropoda, Spinosauridae) from the Cretaceous (Cenomanian) Alcântara Formation, Cajual Island, Brazil. *Anais da Academia Brasileira de Ciencias* 2011;**83**:99–108. https://doi.org/10.1590/s0001-37652011000100006
Klein CG, Longrich NR, Ibrahim N *et al.* A new basal snake from the mid-Cretaceous of Morocco. *Cretaceous Research* 2017;**72**:134–41. https://doi.org/10.1016/j.cretres.2016.12.001
Lacerda MBS, Grillo ON, Romano PSR. Rostral morphology of Spinosauridae (Theropoda, Megalosauroidea): premaxilla shape variation and a new phylogenetic inference. *Historical Biology* 2022;**34**:2089–109. https://doi.org/10.1080/08912963.2021.2000974
Lacerda MBS, Bittencourt JS, Hutchinson JR. Macroevolutionary patterns in the pelvis, stylopodium and zeugopodium of non-avian megalosauroid dinosaurs and their importance for locomotor function. *Royal Society Open Science* 2023;**10**:230481. https://doi.org/10.1098/rsos.230481
Lacerda MBS, Bittencourt JS, Hutchinson JR. Reconstruction of the pelvic girdle and hindlimb musculature of the early tetanurans Piatnitzkysauridae (Theropoda, Megalosauroidea). *Journal of Anatomy* 2024;**244**:557–93. https://doi.org/10.1111/joa.13983
Lakin RJ, Longrich NR. Juvenile spinosaurs (Theropoda: Spinosauridae) from the middle Cretaceous of Morocco and implications for spinosaur ecology. *Cretaceous Research* 2019;**93**:129–42. https://doi.org/10.1016/j.cretres.2018.09.012
Lemierre A, Blackburn DC. A new genus and species of frog from the Kem Kem (Morocco), the second neobatrachian from Cretaceous Africa. *PeerJ* 2022;**10**:e13699. https://doi.org/10.7717/peerj.13699
Machado EB. *Descrição de um Novo Exemplar de Spinosauridae (Dinosauria, Theropoda) da Formação Romualdo (Bacia do Araripe), Nordeste do Brasil*. Rio de Janeiro (RJ): Universidade Federal do Rio de Janeiro. Brazilian Portuguese, 2010.
Madsen JH. Allosaurus fragilis: a revised osteology. *Utah Geological and Mineral Survey Bulletin*, 1976;**109**:1–163.
Maganuco S, Dal Sasso C. The smallest biggest theropod dinosaur: a tiny pedal ungual of a juvenile Spinosaurus from the Cretaceous of Morocco. *PeerJ* 2018;**6**:e4785. https://doi.org/10.7717/peerj.4785
Mahler L. Record of Abelisauridae (Dinosauria: Theropoda) from the Cenomanian of Morocco. *Journal of Vertebrate Paleontology* 2005;**25**:236–9. https://doi.org/10.1671/0272-4634(2005)025[0236:roadtf]2.0.co;2
Malafaia E, Gasulla JM, Escaso F *et al.* New spinosaurid (Theropoda, Megalosauroidea) remains from the Arcillas de Morella Formation (upper Barremian) of Morella, Spain. *Cretaceous Research* 2018;**92**:174–83. https://doi.org/10.1016/j.cretres.2018.08.006
Malafaia E, Gasulla JM, Escaso F *et al.* A new spinosaurid theropod (Dinosauria: Megalosauroidea) from the upper Barremian of Vallibona, Spain: Implications for spinosaurid diversity in the Early Cretaceous of the Iberian Peninsula. *Cretaceous Research* 2020;**106**:104221. https://doi.org/10.1016/j.cretres.2019.104221
Mannion PD, Barrett PM. Additions to the sauropod dinosaur fauna of the Cenomanian (early Late Cretaceous) Kem Kem beds of Morocco: palaeobiogeographical implications of the mid-Cretaceous African sauropod fossil record. *Cretaceous Research* 2013;**45**:49–59. https://doi.org/10.1016/j.cretres.2013.07.007
Marsh OC. Principal characters of American Jurassic dinosaurs. Part I. *American Journal of Science (Series 3)* 1878;**16**:411–6.
Marsh OC. Classification of the Dinosauria. *American Journal of Science (Series 3)* 1881;**s3-23**:81–6. https://doi.org/10.2475/ajs.s3-23.133.81
Mateus O, Estraviz-López D. A new theropod dinosaur from the Early Cretaceous (Barremian) of Cabo Espichel, Portugal: implications for spinosaurid evolution. *PLoS One* 2022;**17**:e0262614. https://doi.org/10.1371/journal.pone.0262614
McFeeters B. New mid-cervical vertebral morphotype of Spinosauridae from the Kem Kem Group of Morocco. *Vertebrate Anatomy Morphology*

Palaeontology 2021;**8**:182–93. https://doi.org/10.18435/vamp29370
McFeeters B, Ryan MJ, Hinic-Frlog S *et al.* A reevaluation of *Sigilmassasaurus brevicollis* (Dinosauria) from the Cretaceous of Morocco. *Canadian Journal of Earth Sciences* 2013;**50**:636–49. https://doi.org/10.1139/cjes-2012-0129
McGowan AJ, Dyke GJ. A surfeit of theropods in the Moroccan Late Cretaceous? Comparing diversity estimates from field data and fossil shops. *Geology* 2009;**37**:843–6. https://doi.org/10.1130/g30188a.1
Milner AC. Fish-eating theropods: a short review of the systematics, biology and palaeobiology of spinosaurs. In: Colectivo Arqueológico-Paleontológico de Salas (ed.), *Actas de las II Jornadas internacionales sobre Paleontología de Dinosaurios y su entorno*. Salas de los Infantes: Colectivo Arqueológico y Paleontológico de Salas, 2003, 129–39.
Nomina Anatomica Veterinaria 2017. Nomina anatomica veterinária.
Novas F, Dalla Vecchia F, Pais D. Theropod pedal unguals from the Late Cretaceous (Cenomanian) of Morocco, Africa. *Revista del Museo Argentino de Ciencias Naturales Nueva Serie* 2005;**7**:167–75.
Paterna A, Cau A. New giant theropod material from the Kem Kem Compound Assemblage (Morocco) with implications on the diversity of the mid-Cretaceous carcharodontosaurids from North Africa. *Historical Biology* 2023;**35**:2036–44. https://doi.org/10.1080/08912963.2022.2131406
Porchetti SDO, Nicosia U, Biava A *et al.* New abelisaurid material from the Upper Cretaceous (Cenomanian) of Morocco. *Rivista Italiana di Paleontologia e Stratigrafia* 2011;**117**:463–72. https://doi.org/10.13130/2039-4942/5986
Rauhut OWM, Pol D. Probable basal allosauroid from the early Middle Jurassic Cañadón Asfalto Formation of Argentina highlights phylogenetic uncertainty in tetanuran theropod dinosaurs. *Scientific Reports* 2019;**9**:1–9. https://doi.org/10.1038/s41598-019-53672-7
Richter U, Mudroch A, Buckley LG. Isolated theropod teeth from the Kem Kem beds (early Cenomanian) near Taouz, Morocco. *Paläontologische Zeitschrift* 2013;**87**:291–309. https://doi.org/10.1007/s12542-012-0153-1
Riff D, Mader B, Kellner AWA *et al.* An avian vertebra from the continental Cretaceous of Morocco, Africa. *Arquivos do Museu Nacional Rio de Janeiro* 2004;**62**:217–23.
Russell DA. Isolated dinosaur bones from the Middle Cretaceous of the Tafilalt, Morocco. *Bulletin du Muséum National d'Histoire Naturelle, 4 série–section C–Sciences de la Terre, Paléontologie, Géologie, Minéralogie* 1996;**18**:349–402.
Sales MA, Schultz CL. Spinosaur taxonomy and evolution of craniodental features: Evidence from Brazil. *PLoS One* 2017;**12**:e0187070. https://doi.org/10.1371/journal.pone.0187070
Sampson SD, Witmer LM. Craniofacial Anatomy of *Majungasaurus crenatissimus* (Theropoda: Abelisauridae) from the Late Cretaceous of Madagascar. *Journal of Vertebrate Paleontology* 2007;**27**:32–104. https://doi.org/10.1671/0272-4634(2007)27[32:caomct]2.0.co;2
Schade M, Rauhut OWM, Foth C *et al.* A reappraisal of the cranial and mandibular osteology of the spinosaurid *Irritator challengeri* (Dinosauria: Theropoda). *Palaeontologia Electronica* 2023;**26**:a17. https://doi.org/10.26879/1242
Sereno PC, Brusatte SL. Basal abelisaurid and carcharodontosaurid theropods from the lower cretaceous Elrhaz formation of Niger. *Acta Palaeontologica Polonica* 2008;**53**:15–46. https://doi.org/10.4202/app.2008.0102
Sereno PC, Larsson HCE. Cretaceous crocodyliforms from the Sahara. *ZooKeys* 2009;**28**:1–143. https://doi.org/10.3897/zookeys.28.325
Sereno PC, Dutheil DB, Iarochene M *et al.* Predatory dinosaurs from the Sahara and Late Cretaceous faunal differentiation. *Science* 1996;**272**:986–91. https://doi.org/10.1126/science.272.5264.986
Sereno PC, Beck AL, Dutheil DB *et al.* A long-snouted predatory dinosaur from Africa and the evolution of Spinosaurids. *Science* 1998;**282**:1298–302. https://doi.org/10.1126/science.282.5392.1298
Sereno PC, Wilson JA, Conrad JL. New dinosaurs link southern landmasses in the Mid–Cretaceous. *Proceedings of the Royal Society of London. Series B: Biological Sciences* 2004;**271**:1325–30. https://doi.org/10.1098/rspb.2004.2692
Sereno PC, Myhrvold N, Henderson DM *et al. Spinosaurus* is not an aquatic dinosaur. *eLife* 2022;**11**:e80092. https://doi.org/10.7554/eLife.80092
Smith JB, Lamanna MC, Mayr H *et al.* New information regarding the holotype of *Spinosaurus aegyptiacus* Stromer, 1915. *Journal of Paleontology* 2006;**80**:400–6. https://doi.org/10.1666/0022-3360(2006)080[0400:nirtho]2.0.co;2
Smith RE, Ibrahim N, Longrich N *et al.* The pterosaurs of the Cretaceous Kem Kem Group of Morocco. *PalZ* 2023a;**97**:519–68. https://doi.org/10.1007/s12542-022-00642-6
Smith RE, Martill DM, Longrich N *et al.* Comparative taphonomy of Kem Kem Group (Cretaceous) pterosaurs of south-east Morocco. *Evolving Earth* 2023b;**1**:100006. https://doi.org/10.1016/j.eve.2023.100006
Smyth RS, Ibrahim N, Kao A *et al.* Abelisauroid cervical vertebrae from the Cretaceous Kem Kem beds of Southern Morocco and a review of Kem Kem abelisauroids. *Cretaceous Research* 2020a;**108**:104330. https://doi.org/10.1016/j.cretres.2019.104330
Smyth RS, Ibrahim N, Martill DM. *Sigilmassasaurus* is *Spinosaurus*: a reappraisal of African spinosaurines. *Cretaceous Research* 2020b;**114**:104520. https://doi.org/10.1016/j.cretres.2020.104520
Souza LG, Pêgas RV, Lacerda MBS *et al.* Tales of long faces: piscivorous Archosauriformes and the evolutionary ways to form a fisher. In: HN Woodward, JO Farlow (eds), *Ruling Reptiles: Crocodylian Biology and Archosaur Paleobiology*. Bloomington: Indiana University Press, Indiana, 2023, 215–39. https://doi.org/10.2307/jj.6047951.13
Souza-Júnior AL, Candeiro CRDA, Vidal LDS *et al.* Abelisauroidea (Theropoda, Dinosauria) from Africa: a review of the fossil record. *Papéis Avulsos de Zoologia* 2023;**63**:e202363019. https://doi.org/10.11606/1807-0205/2023.63.019
Stovall JW, Langston W. *Acrocanthosaurus atokensis*, a new genus and species of Lower Cretaceous Theropoda from Oklahoma. *The American Midland Naturalist* 1950;**43**:696–728. https://doi.org/10.2307/2421859
Stromer E. Ergebnisse der Forschungsreisen Prof. E. Stromers in den Wüsten Ägyptens. II. Wirbeltier-Reste der Baharîje-Stufe (unterstes Cenoman). 3. Das Original des Theropoden *aegyptiacus* nov. gen., nov. spec. *Abhandlungen der Königlich Bayerischen Akademie der Wissenschaften, Mathematisch-physikalische Klasse* 1915;**28**:1–32.
Stromer E. Wirbeltier-Reste der Baharije-Stufe (unterstes Cenoman). 10. Ein Skelett-Rest von *Carcharodontosaurus* nov. gen. *Abhandlungen der Königlich Bayerischen Akademie der Wissenschaften, Mathematisch-naturwissenschaftliche Abtellung* 1931;**10**:1–21.
Sues H-D, Frey E, Martill DM *et al. Irritator challengeri*, a spinosaurid (Dinosauria: Theropoda) from the Lower Cretaceous of Brazil. *Journal of Vertebrate Paleontology* 2002;**22**:535–47. https://doi.org/10.1671/0272-4634(2002)022[0535:icasdt]2.0.co;2
Taquet P, Russell DA. New data on spinosaurid dinosaurs from the Early Cretaceous of the Sahara. *Comptes Rendus de l'Académie des Sciences - Series IIA - Earth and Planetary Science* 1998;**327**:347–53. https://doi.org/10.1016/s1251-8050(98)80054-2
Vullo R. A new species of *Lapparentophis* from the mid-Cretaceous Kem Kem beds, Morocco, with remarks on the distribution of lapparentophiid snakes. *Comptes Rendus Palevol* 2019;**18**:765–70. https://doi.org/10.1016/j.crpv.2019.08.004
Witmer LM. The extant phylogenetic bracket and the importance of reconstructing soft tissues in fossils. In Thomason JJ (eds), *Functional Morphology in Vertebrate Paleontology*. Cambridge University Press, 1995, 19–33.
Zanno LE, Makovicky PJ. Neovenatorid theropods are apex predators in the Late Cretaceous of North America. *Nature Communications* 2013;**4**:2827. https://doi.org/10.1038/ncomms3827